ADDED MASS OF A CIRCULAR CYLINDER UNDER A FREE SURFACE

Richard Leon Gosselin

NAVAL POSTGRADUATE SCHOOL
Monterey, California

THESIS

Added Mass of a Circular Cylinder
Under a Free Surface

by

Richard Leon Gosselin

Thesis Advisor: C. J. Garrison

December 1971

Added Mass of a Circular Cylinder Under a Free Surface

by

Richard Leon Gosselin
Lieutenant, United States Navy
B.S., University of North Carolina at Chapel Hill, 1964

Submitted in partial fulfillment of the
requirement for the degree of

MASTER OF SCIENCE IN MECHANICAL ENGINEERING

from the

NAVAL POSTGRADUATE SCHOOL
December 1971

ABSTRACT

When a circular cylinder is immersed in a fluid of infinite extent and oscillated in such a manner that drag effects are negligible, it is well known that the closed form solution gives an added mass coefficient of 1.0. However, when boundaries are placed in proximity to the cylinder, and the cylinder oscillated parallel to the boundary, the added mass varies from the classical result. The forces acting on the cylinder in the latter case are dependent upon the proximity of the boundaries as well as the frequency of oscillation.

It was the purpose of this study to experimentally determine the total force on such a cylinder in proximity to an impermeable bottom surface and under a free surface and to relate this force to the added mass coefficient. Experimental data was reduced using a computer program and the results presented graphically as a function of dimensionless parameters.

TABLE OF CONTENTS

LIST OF TABLES

The above tables are presented in Appendix B

LIST OF FIGURES

NOMENCLATURE

Symbol	Description
$\bar{a}$	Radius of Circular Cylinder
d	Relative Depth of Submergence
$\bar{d}$	Depth of Submergence of Cylinder
F	Total Maximum Force Per Unit Length
g	Acceleration of Gravity
h	Relative Water Depth
$\bar{h}$	Water Depth
PA	Phase Angle
WH	Waveheight
x	Relative Displacement
X	Half Amplitude of Cylinder Oscillation
ν	Dimensionless Frequency Parameter
ρ	Water Density
σ	Circular Frequency of Cylinder Oscillation
μ	Water Viscosity

DIMENSIONLESS NOTATION

$F/\rho g \pi \bar{a}^2 \sigma^2 X$	Force Coefficient
$\sigma^2 \bar{a}/g = \nu$	Frequency Parameter
$\bar{d}/\bar{a} = d$	Relative Depth of Submergence
$\bar{h}/\bar{a} = h$	Relative Water Depth
$X/\bar{a} = x$	Relative Displacement
$2\rho \bar{a} X \sigma / \mu$	Reynold's Number

ACKNOWLEDGEMENTS

The author wishes to acknowledge the following members of the Department of Mechanical Engineering Staff, Messrs. K. Mothersell, G. Baxter, T. Christian, and Mrs. V. Culley for their help in procurement and construction of the apparatus.

The author gratefully acknowledges the patient encouragement and supervision of Dr. C. J. Garrison of the Naval Postgraduate School, his advisor.

The author's wife, Joan, has faithfully tolerated him throughout the development of this work. Her constant encouragement is only one of the many reasons that she deserves a very special thank you.

I. INTRODUCTION

During the past two decades, many new submarine structures, such as pipelines, oil storage tanks and large aquaducts have been either sunk or moored on the continental shelf. Consequently, the calculation of the forces exerted on such objects is of practical importance.

In an early paper [1], Stokes showed that the expression for the force on a pendulum-like system oscillating in an infinite fluid was both acceleration and velocity dependent.

In more recent years, Morison, et al, [2], from an investigation of wave forces exerted on piles, showed that when the characteristic dimension of a body, i.e., pile diameter, was small compared to wave length, the force consisted of both a drag and an inertial term. However, the coefficient of each of these terms depends upon the geometry of the object in question, the amplitude of the fluid motion, the proximity of a free surface, and the proximity of an impermeable bottom surface.

Several investigations have been conducted since Morison's work, which have dealt with sinusoidal flow about various objects. Keulegan and Carpenter [3] performed an experimental study with cylinders and plates in a rectangular tank in which a standing wave was generated in water. Forces on the submerged bodies were measured with a dynamometer. Inertial and drag coefficients were correlated with a dimensionless "period parameter" for both unseparated and separated flow, the period parameter being proportional to the relative displacement of the surrounding fluid.

Heinzer [4] carried out a visual study of the flow field characteristics of a cylinder sinusoidally oscillated in a still fluid. Flow patterns included laminar boundary layer, symmetric separation, and Karman vortex street. Heinzer's major conclusion was that wake characteristics were primarily dependent upon the relative amplitude of oscillates. A consideration of this type was used in the study which follows. Small amplitude oscillations were utilized at various frequencies to insure unseparated flow.

Sarpkaya and Garrison [5] studied constantly accelerated, unidirectional flow past a circular cylinder. Forces were measured experimentally and the nature of the flow determined visually. Force coefficients were calculated as functions of the relative displacement of the cylinder. It was shown that the total resistance as well as the drag and inertial forces are representable as functions of the relative displacement of the fluid.

Ward and Dalton [6] analyzed the forces exerted on a cylinder in a purely sinusoidal flow field in which symmetrically located vortex pairs were developed. Forces acting on the cylinder were calculated using Bryson's [7] potential flow model including a pair of vortices but no attempt was made to verify these forces experimentally.

Later Dalton and Hamann [8] conducted an experimental investigation of a sinusoidally osciallating cylinder in a quiescent fluid in an attempt to represent a sinusoidal wave moving past a single, fixed platform leg. The conclusions drawn from their investigation were mostly qualitative.

The purpose of this study was to provide a correlation between the added mass coefficient and appropriate dimensionless parameters. A right circular cylinder was oscillated in a quiescent fluid at amplitudes which insured unseparated flow. The results are presented in dimensionless form as a function of a dimensionless frequency parameter, relative water depth, relative depth of submergence, and relative amplitude of oscillation.

II. THEORETICAL CONSIDERATIONS

A schematic representation of the problem is shown in Figure (1). A right circular cylinder of radius $\bar{a}$ was submerged to a depth $\bar{d}$ in water of depth $\bar{h}$. The cylinder was oscillated sinusoidally at a circular frequency σ with half amplitude of oscillation X Of primary interest was the total maximum force per unit length F exerted by the water on the cylinder, the phase of this force and the amplitude of the generated waves.

The complete theoretical solution to the problem is complicated, even when the amplitude of oscillation is kept small enough to justify an assumption that the flow remained unseparated. Therefore, in order to make some headway a dimensional analysis was applied to the problem. It is known "a priori" that the maximum force per unit length of cylinder has the following functional dependence.

$$F = f_1(\bar{h},\bar{d},\bar{a},\sigma,X,\rho,g,\mu) \qquad (1)$$

where $\bar{h}$ denotes the water depth, $\bar{d}$ the depth of submergence, $\bar{a}$ the cylinder radius, σ the circular frequency of the imposed motion, X the half amplitude of the imposed motion, ρ the water density, g the acceleration of gravity, and μ the water viscosity.

Dimensional analysis of the physical quantities of Equation (1) resulted in the following dimensionless groups

$$F/\rho g\pi\bar{a}^2\sigma^2X = f_2\left(\frac{\sigma^2\bar{a}}{g}, \frac{\bar{d}}{\bar{a}}, \frac{\bar{h}}{\bar{a}}, \frac{X}{\bar{a}}, \frac{2\rho\bar{a}X\sigma}{\mu}\right) \qquad (2)$$

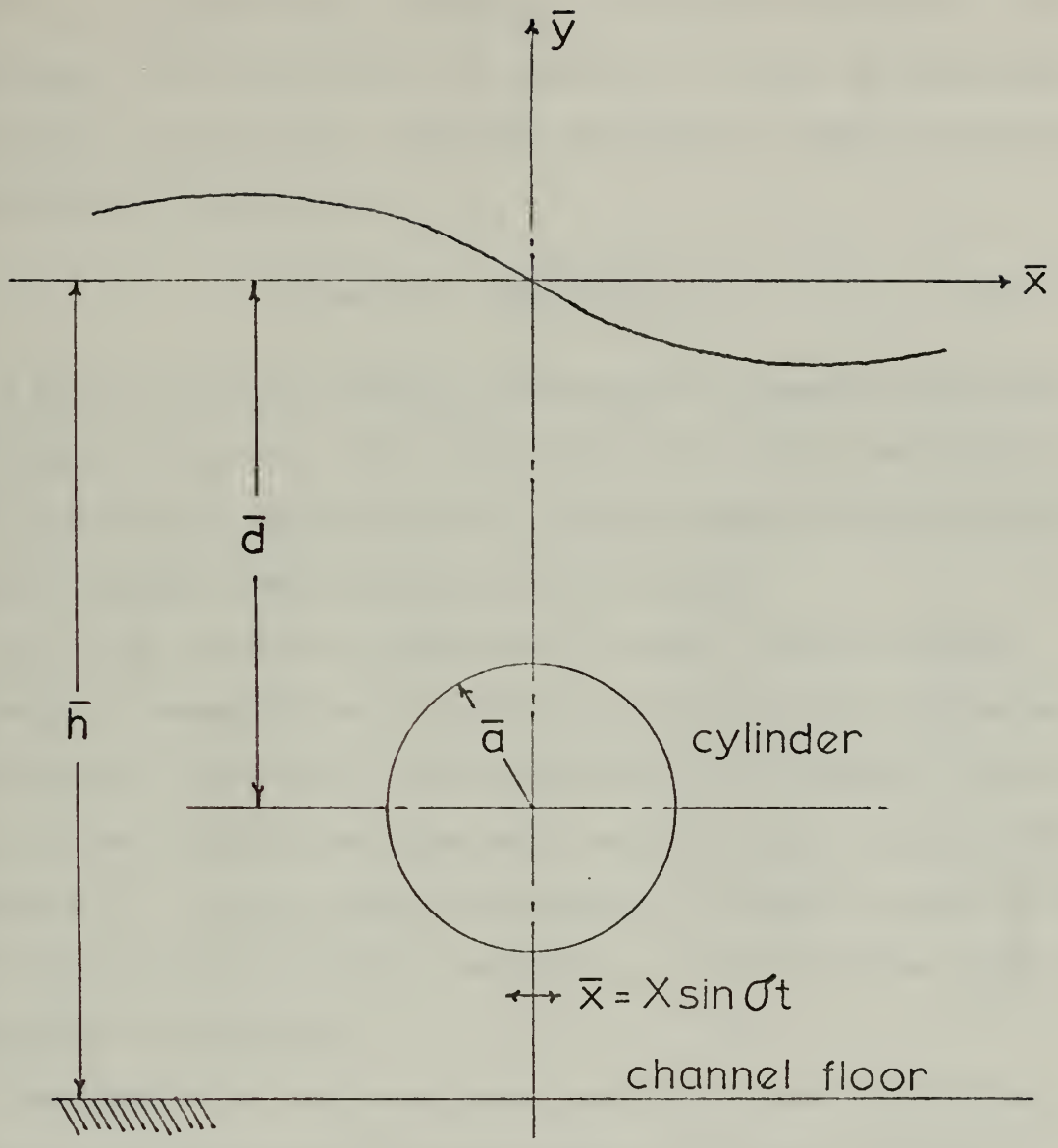

FIGURE 1. DEFINITION SKETCH

where $\frac{2\rho\bar{a}X\sigma}{\mu}$ is the well known Reynold's number representing the ratio of inertial to viscuous forces. Since the cylinder was oscillated at small amplitudes it was assumed that flow around the cylinder was unseparated and viscous forces small. Therefore, the Reynold's number was disregarded and Equation (2) written as

$$F/\rho g\pi\bar{a}^2\sigma^2 X = f_3\left(\frac{\sigma^2 a}{g}, \frac{\bar{d}}{\bar{a}}, \frac{\bar{h}}{a}, \frac{X}{\bar{a}}\right) \qquad (3)$$

A second reason for ignoring a dependence upon Reynold's number was provided by Heinzer [4]. His visual studies showed that wake characteristics were primarily dependent upon the relative amplitude of oscillation and that Reynold's number effects were not evident.

As long as the relative displacement is small, the flow remains essentially unseparated and, accordingly, the force is also independent of the relative amplitude. The independence of the force from this parameter for small values was demonstrated experimentally by Keulegan and Carpenter [3]. In the present investigation, no attempt was made to study the effects of this parameter; consequently, it was held fixed at $\frac{X}{\bar{a}} = 0.1$ throughout the experiment.

The objective of this experimental work was to show a correlation between the dimensionless force coefficient on the left hand side of Equation (3) and the dimensionless parameters on the right hand side.

III. EXPERIMENTAL INVESTIGATION

A. APPARATUS

1. Wave Channel

The wave channel was designed and built by Shiller [9] for an earlier thesis. The channel was designed with a rectangular cross section two feet deep and fifteen inches wide. It was fabricated in sections, each section consisting of two vertical walls and one horizontal floor member. The vertical walls were stiffened by use of three four foot long 2 x 4's attached to 3/4 inch x 8 foot x 3 foot sheets of plywood at the ends and middle of the longest dimension. The channel floor member was composed of two 15 inch x 8 foot long plywood sheets separated by a 1 inch x 4 inch strip around the edge. The bottom and side members for-formed the basic channel cross section. The bottom and side members were mated together with 3/8 inch threaded rods. Six of these 8 foot sections were sealed and bolted together to form a 48 foot long channel. Squareness of the channel cross sections was maintained by use of spacers placed between the stiffened members near the floor and across the top.

One end of the channel was fitted with a wave generating mechanism which was not used in this investigation.

At a location 30 feet from the wave generator end of the channel, a three foot wide plexiglass observation window extending the full height of the channel was installed in both walls as shown in Figure (2). The test cylinder was sinusoidally oscillated at a position near one end of the plexiglass window.

FIGURE 2. WAVE CHANNEL OBSERVATION WINDOW

The generated waves were dissipated on a beach structure located at each end of the channel. The beach as shown in Figure (3) consisted of three layers of perforated stainless steal sheeting. Layer separation and structural strength were provided by 2 x 4 runners with their largest cross sectional dimension perpendicular to the sheeting. The slope of the beach was 6:1.

2. Carriage and Driving Mechanism

The driving mechanism as shown in Figure (4) consisted of a variable speed transmission driven by a two-horsepower inductance motor. The motor and transmission were mounted on a 3/4 inch steel plate which was positioned and bolted to the top of the channel. The plate was further braced using 1/2 inch angle iron supports which were bolted across the top of the channel and diagonally to the channel side wall. The variable speed transmission provided an output shaft speed range extending from 22 to 180 rpm which in turn provided dimensionless frequency parameters of from about 0.04 with a six inch diameter cylinder to about 1.7 with a four inch diameter cylinder.

The output shaft of the transmission was fitted with a face plate. The face plate as shown in Figure (5) was connected to the drive rod through a bolt and slot assembly which provided a drive rod stroke which could be varied between zero and six inches.

The carriage as shown in Figure (6) provided a movable mounting platform capable of being positioned over the top of the wave channel. The carriage was driven sinusoidally by the driving mechanism at amplitudes of about 10% of the cylinder diameter.

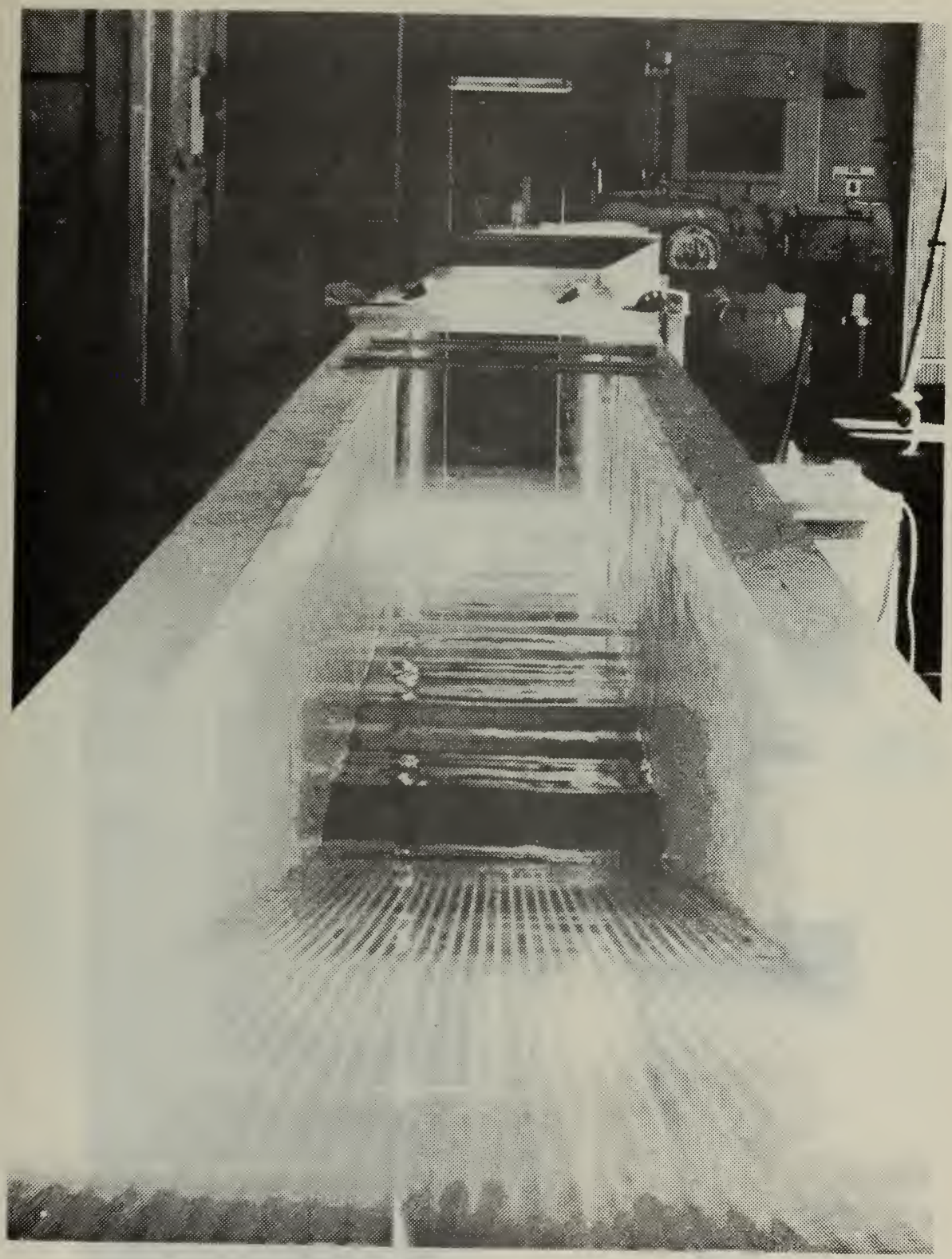

FIGURE 3. BEACH STRUCTURE

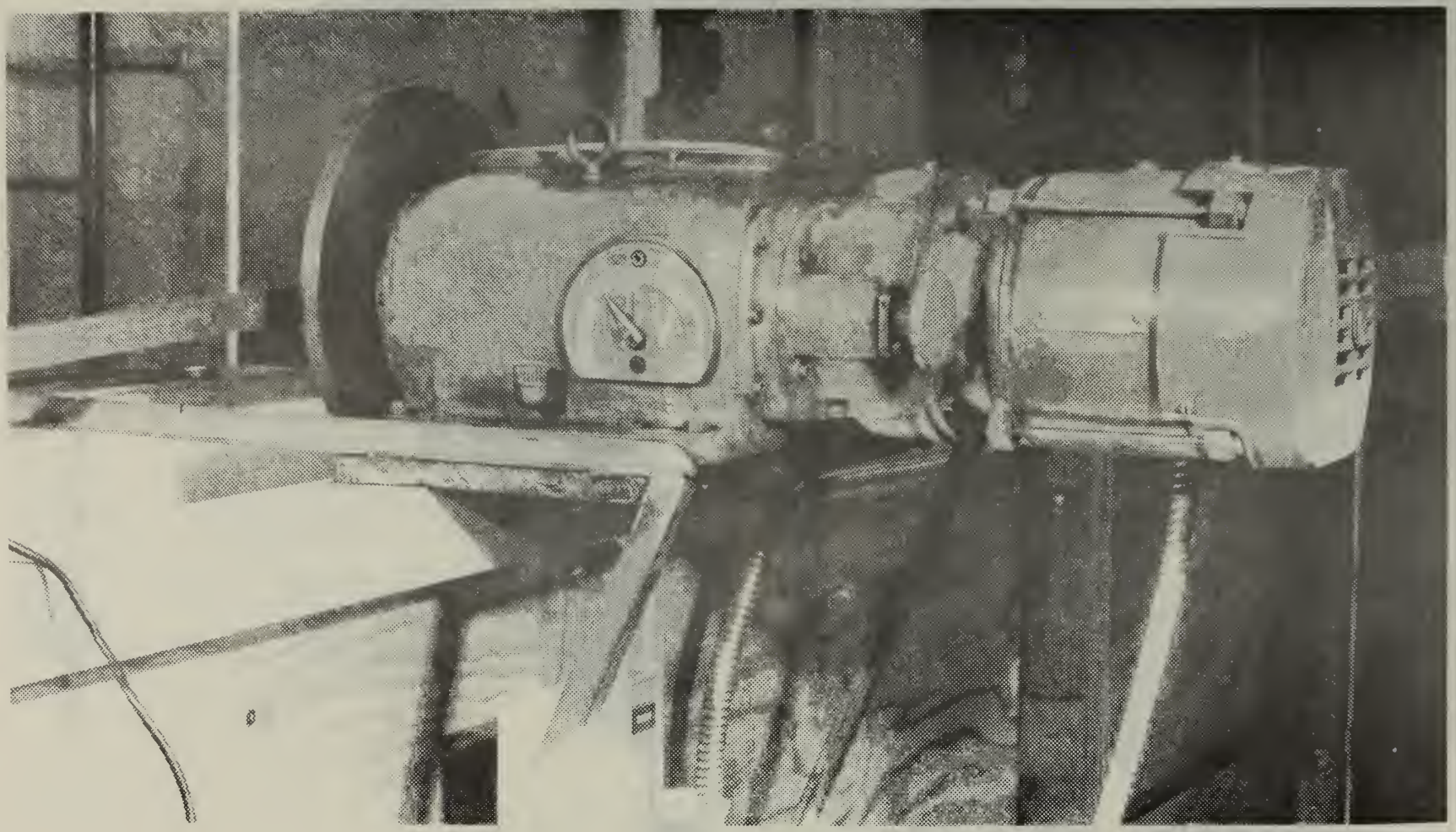

FIGURE 4. DRIVING MOTOR AND TRANSMISSION

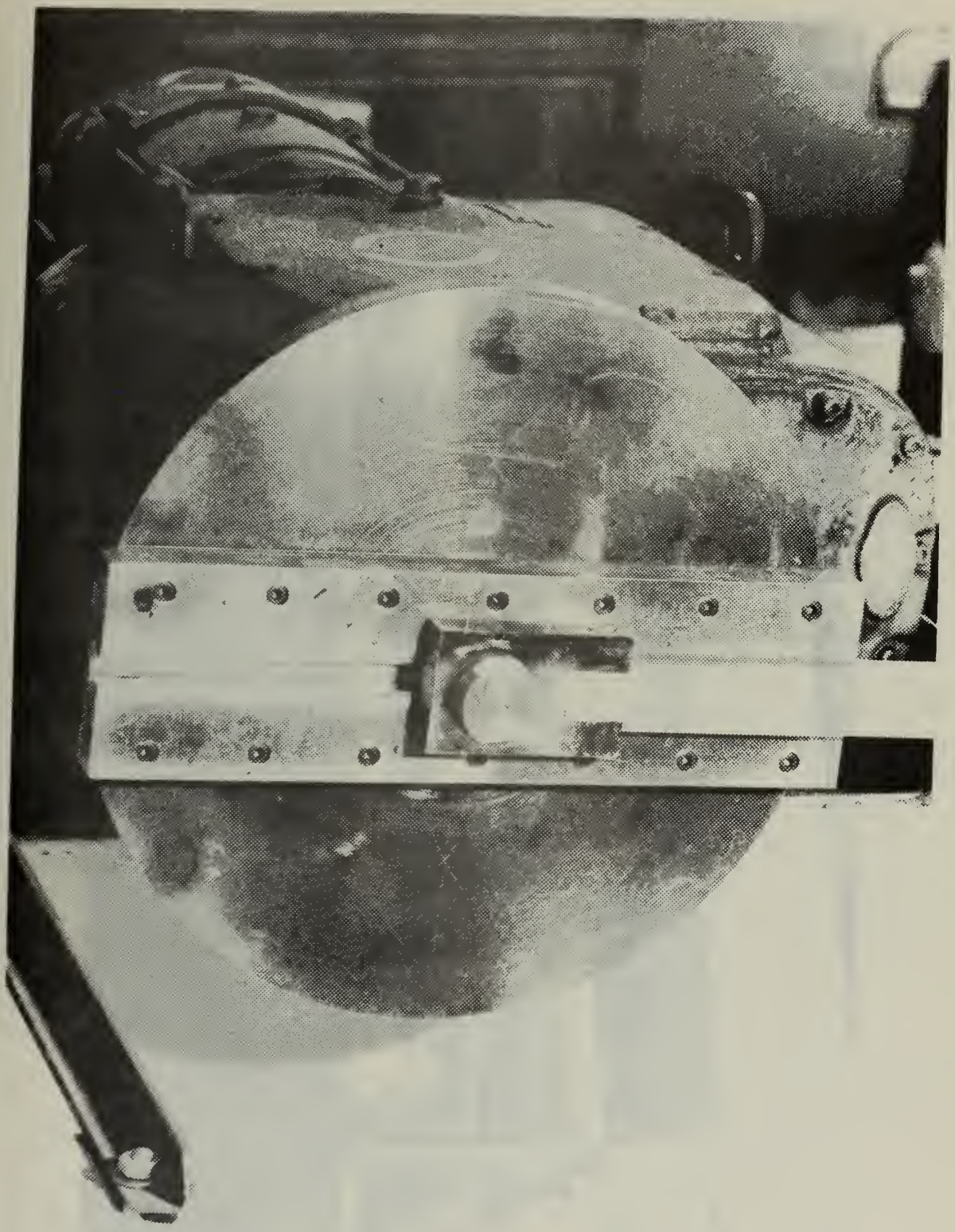

FIGURE 5. FACE PLATE WITH BOLT AND SLOT ASSEMBLY

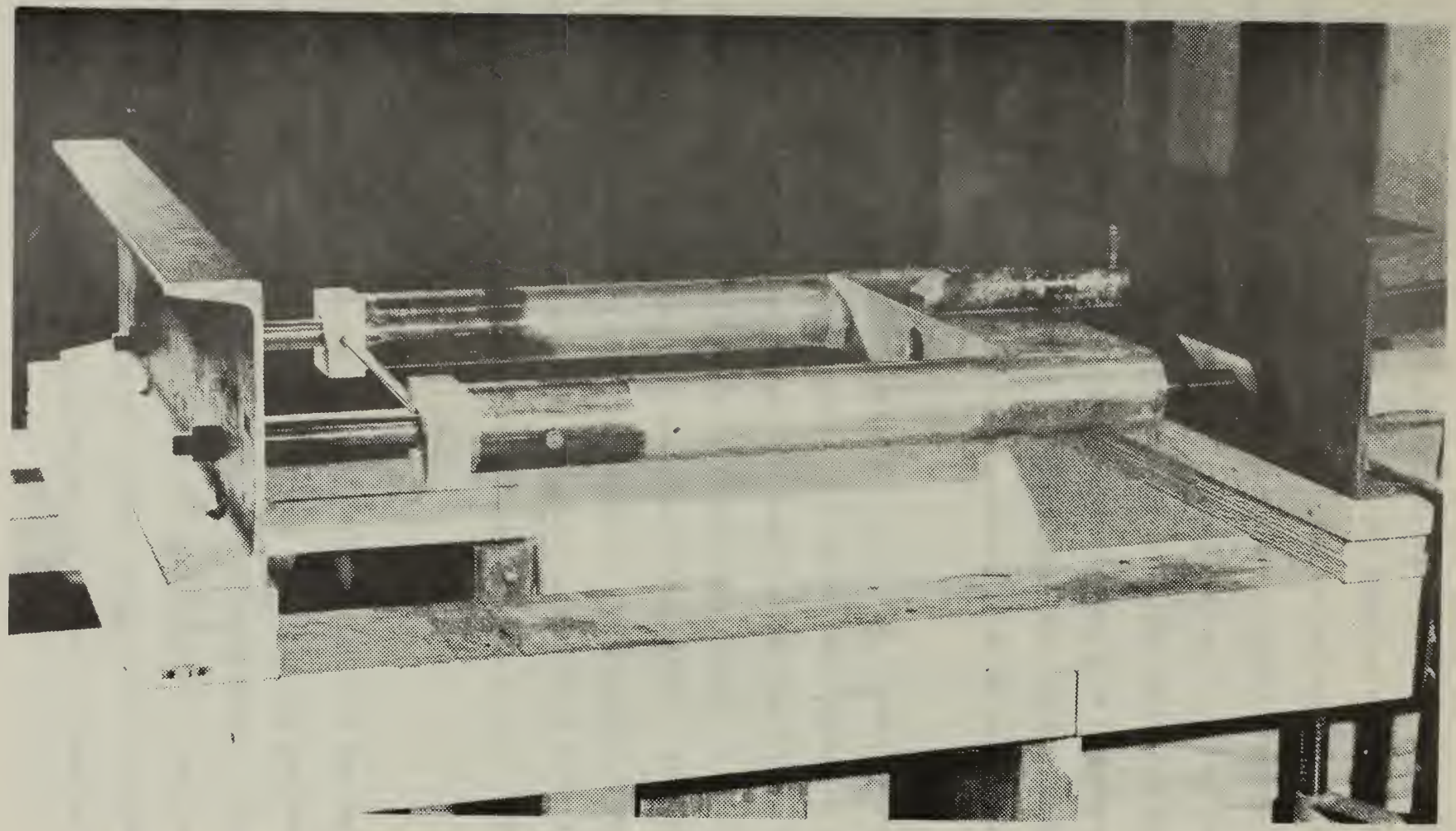

FIGURE 6. CARRIAGE

The carriage consisted of a U-shaped, welded aluminum platform fitted with four 3/4 inch linear bearings. The sides of the platform were constructed of two inch OD aluminum pipe fitted at each end with aluminum bearing blocks designed to accommodate the linear bearings. The structural transverse member of the carriage was a 2 x 3 inch aluminum box which was welded to the pipes at one end. The cantilever beam used to measure forces on the cylinder was mounted on this transverse member. At the opposite end of the aluminum pipe, the bearing blocks were connected by a 1/2 inch diameter transverse shaft which accommodated the cylinder holding and balancing jig.

The U-shaped platform was mounted through the linear bearings onto two case-hardened 3/4 inch shafts. The shafts were supported and held parallel by two six inch channel end pieces which transversed the wave channel. The six inch channel end pieces were clamped to the top of the wave channel at a position over the observation window. The driving mechanism oscillated the carriage sinusoidally. The driving rod was connected to the 2 x 3 inch aluminum transverse member by a stiff link which passed through an accommodation hole drilled through the intervening six inch channel end piece.

3. Cylinder Holding and Balancing Jig

The cylinder holding and balancing jig consisted of two long arms pivoted near their centers as shown in Figure (7). The jig was designed to hold the test cylinder at the desired depth of submergence. It was designed to have as low a moment of inertia with respect to its pivot point as possible in order to maintain a high system natural frequency while having adequate sensitivity of force measurement. A counter balance

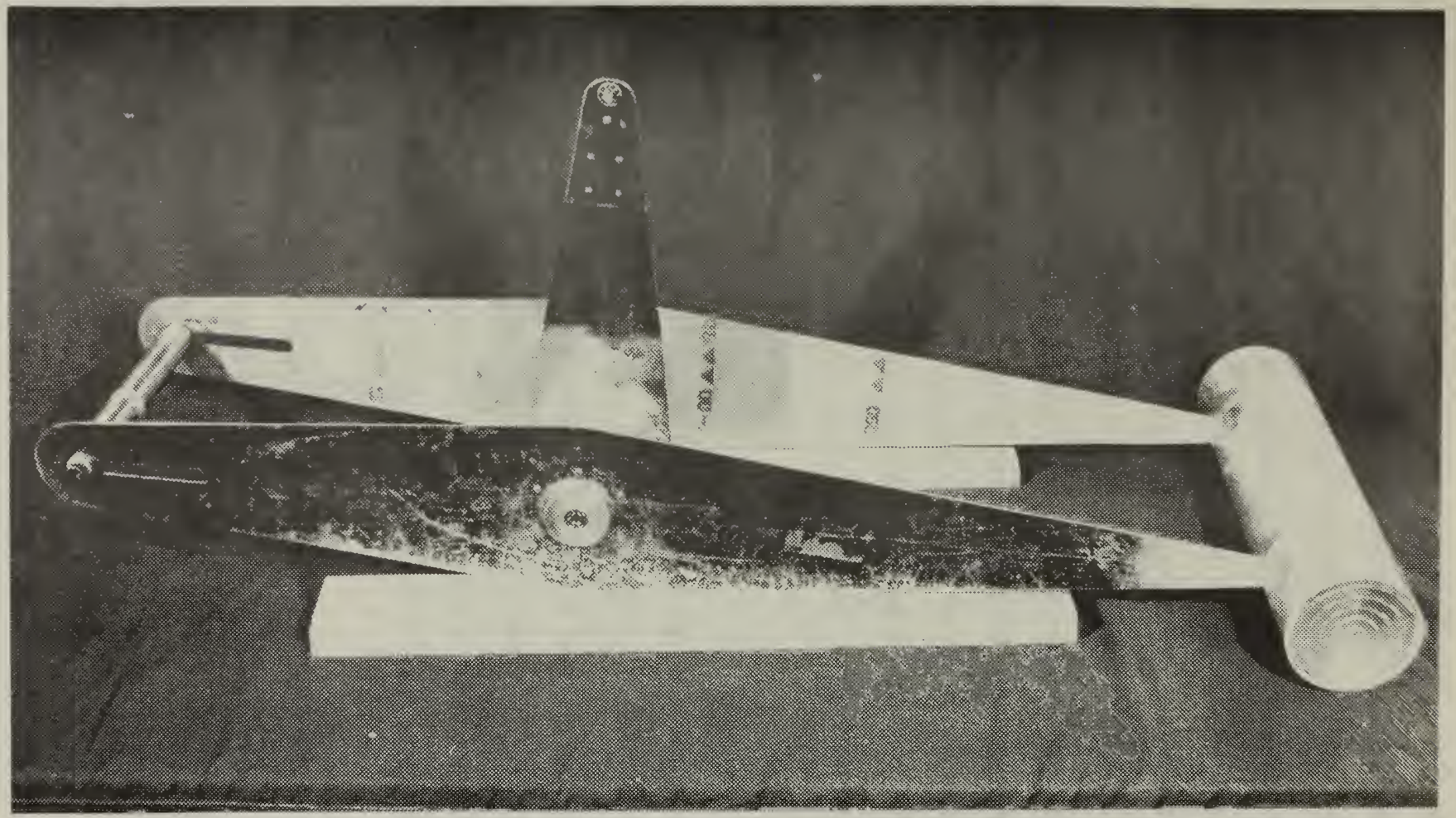

FIGURE 7. CYLINDER HOLDING AND BALANCING JIG WITH CYLINDER IN PLACE

was placed on the arms opposite the cylinder and adjusted so that the center of gravity of the system was at the pivot point. As a result of this balance adjustment the only force (or moment) acting on the arms was that due to the water; all other inertial loads were balanced out.

A twelve inch long arm was welded at the longitudinal center of the center drum and functioned to convert a torque about the rotational center of the drum to a linear force. This force acted, through a ball bearing linkage, on a small cantilever beam. Two attachment points on the beam were provided so that a large range of forces could be measured without overstressing the beam. The stiffness of the beam was adjusted for adequate sensitivity while providing the maximum possible system natural frequency. The design natural frequency was approximately 5.0 times the maximum forcing frequency.

4. Beam and Link

The beam and link assembly as shown in Figure (8) functioned to rigidly connect the cylinder holding and balancing jig to the carriage. Strain gauges were applied to the beam to provide a means of measuring forces imposed upon the cylinder and transmitted mechanically through the assembly. The strain gauge output was calibrated using dead weight loads applied horizontally to the cylinder through a pully arrangement.

5. Test Cylinders

Two cylinders as shown in Figure (9) were constructed to provide maximum flexibility in testing over a wide range of dimensionless frequency parameters. A four inch OD cylinder was constructed of thin-walled aluminum tubing and a six inch OD cylinder was constructed of plexiglass. The cylinders were slotted to accommodate one end of the

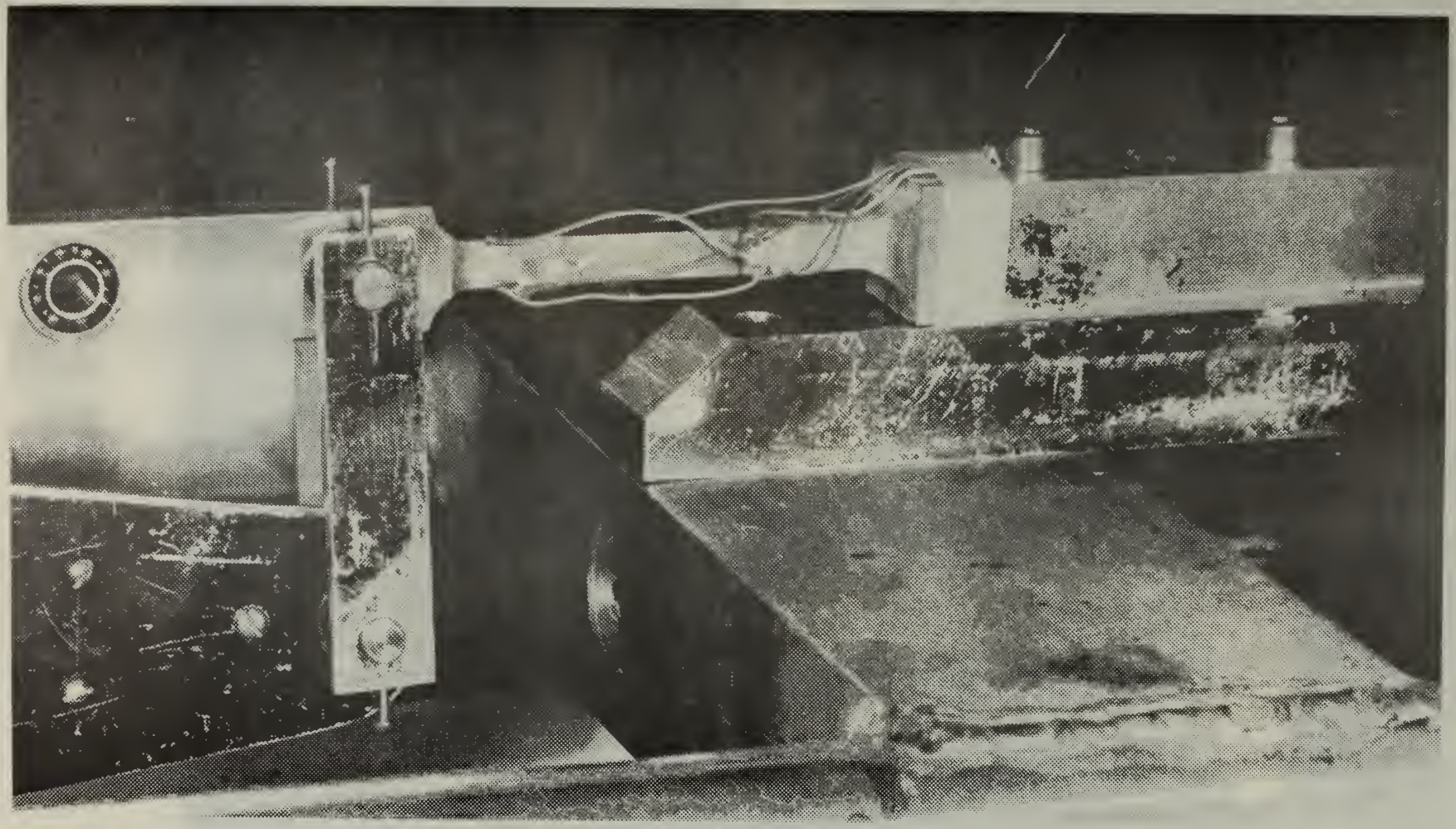

FIGURE 8. BEAM AND LINK

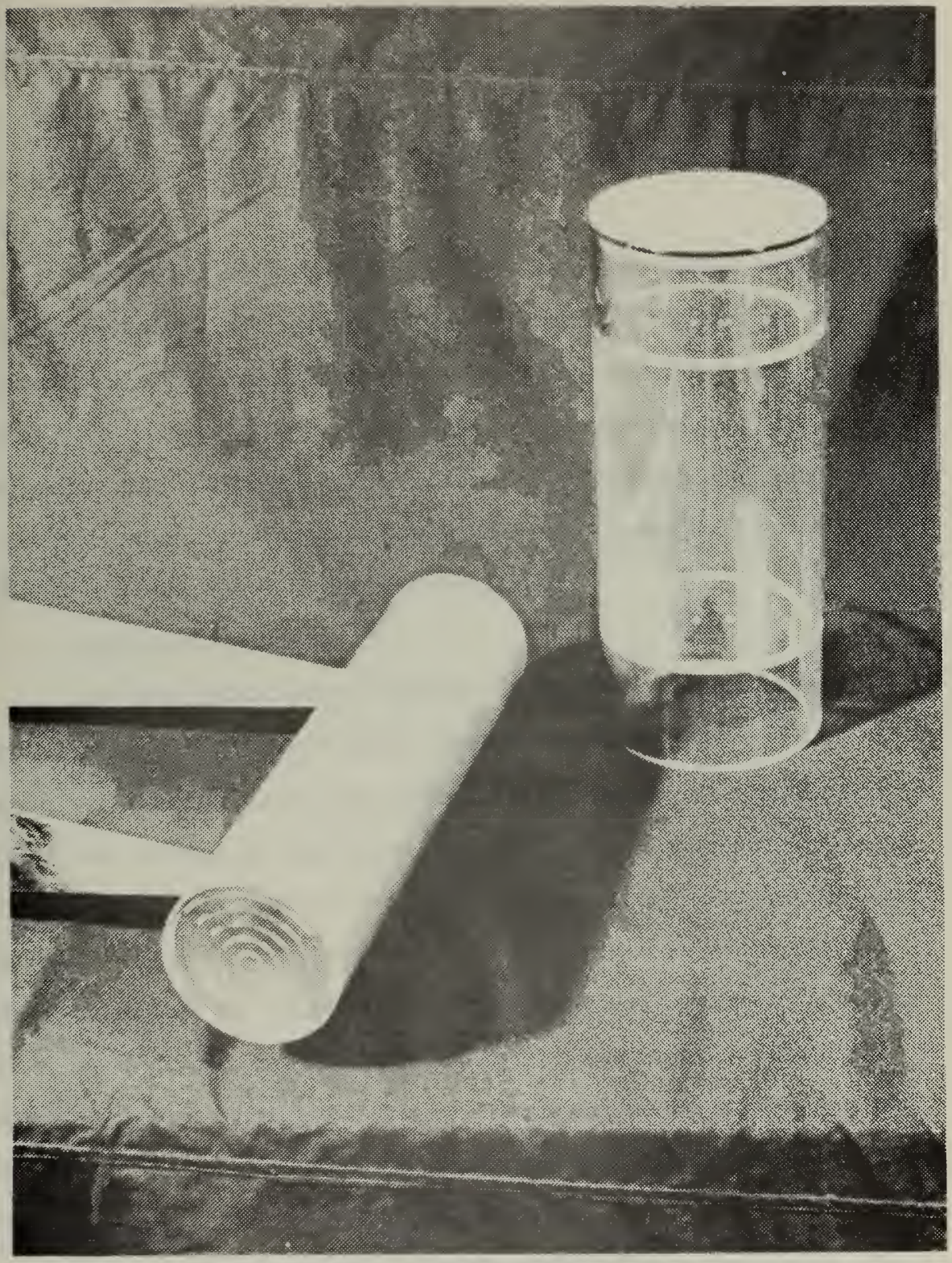

FIGURE 9. TEST CYLINDERS

holding and balancing arms. Bulkheads were placed adjacent to the slots to provide an attachment point for the ends of the arms. Silicone sealant was used to seal the cylinder against leakage after the arms were attached. This allowed the cylinder to be unflooded resulting in a minimum fixed mass.

End pieces as shown in Figure (10) were constructed of plexiglass for each cylinder. The end pieces were fitted into the ends of the cylinders with 1/8 inch "O" rings to provide the necessary seal. End pieces were "dished" on the inner surface to reduce weight. The outer surfaces of the end pieces had a modified labyrinth seal cut into the face to prevent water from flowing between the wave channel wall and the cylinder end when the cylinder was oscillated.

6. Wave Height Gauge

The wave height gauge, as shown in Figure (11), consisted of a small diameter aluminum rod which acted as the basic frame to which a plexiglass mounting table was attached. The elements of a Wheatstone bridge were mounted on this table, and two 30 gauge copper wires spaced 1/2 inch apart were extended from the table and attached to an insulator mounted at the end of the aluminum rod. The other end of the rod was fitted to a block and stand which allowed the gauge to travel ±6 inches in the vertical direction. The block and stand provided a convenient, accurate means of calibration through adjustment of the submergence of the wires. The complete unit was positioned over the channel and centered at about five feet from the carriage.

The wave height gauge was of the parallel wire resistance type. The gauge operated on the principle that the conductance between two parallel submerged wires varies proportionately to the length of wire

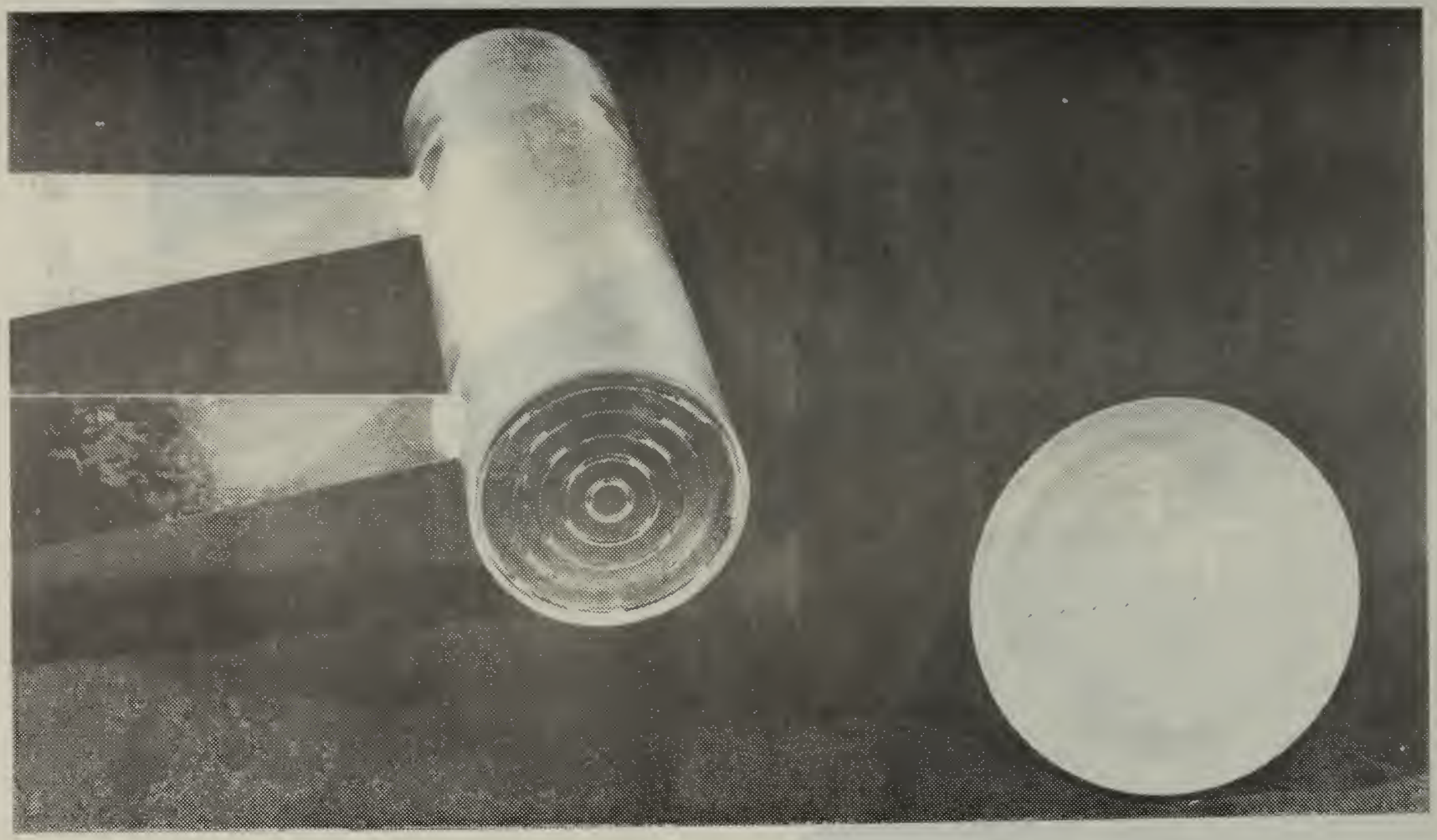

FIGURE 10. END PIECES

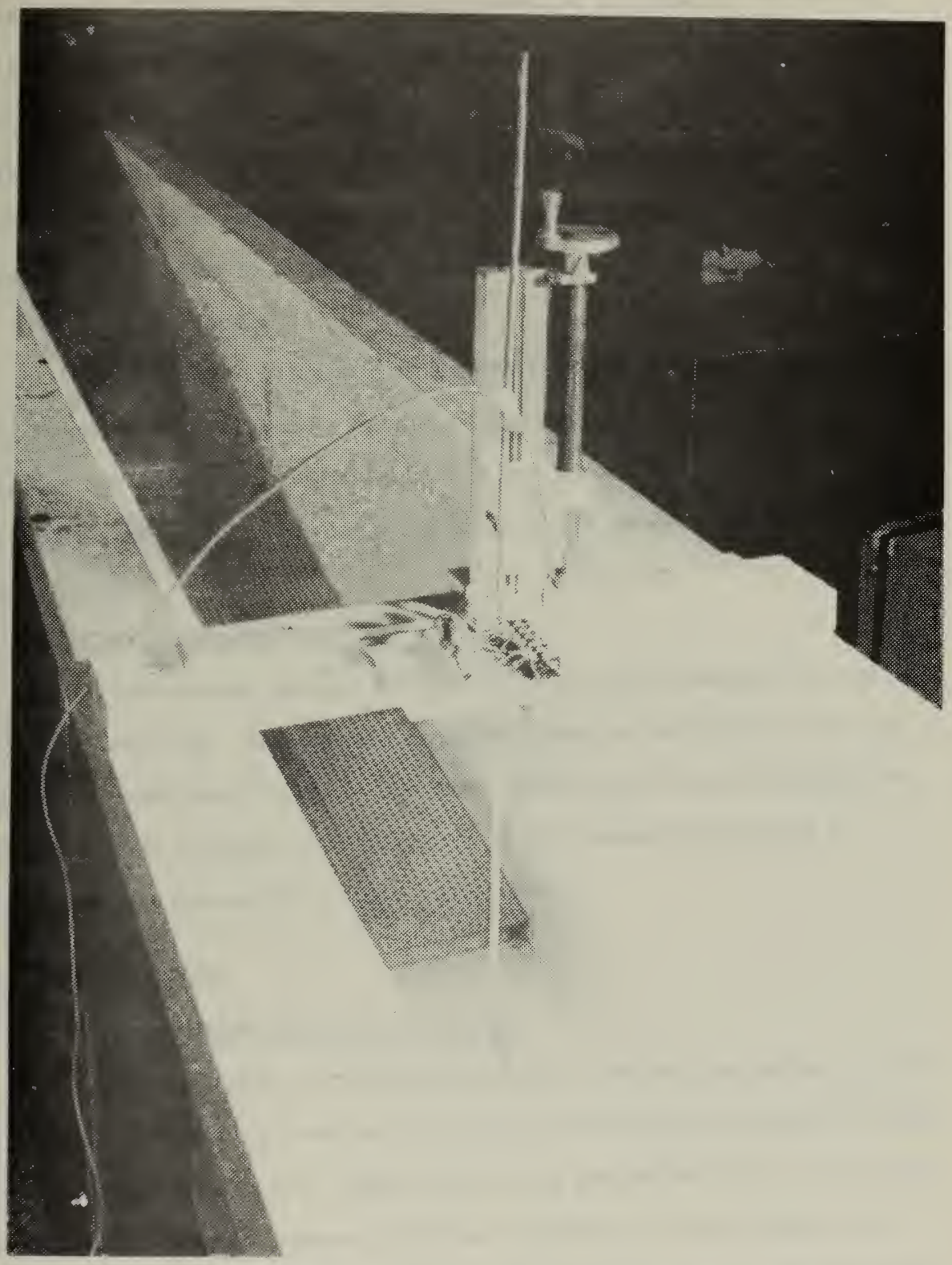

FIGURE 11. WAVE HEIGHT GAUGE

submerged. The wave height gauge was connected in parallel to one leg of a Wheatstone bridge as shown in Figure (12). To compensate for the inability of the carrier preamplifier to offset the resistance of the immersed parallel wires, an external fixed resistance was connected across an opposite leg of the bridge. The Wheatstone bridge was connected with shielded cable to a carrier preamplifier and recorder.

7. R. P. M. Switch

The rpm switch as shown in Figure (13) was designed to measure the frequency of the motion imposed on the cylinder. At the end of each stroke, the switch was closed and the event recorded on the chart. This mark was also used to determine the phase shift between the force and acceleration.

8. Carrier Preamplifier and Recorder

A two-channel Hewlett Packard 8805B carrier preamplifier and recorder was used. One channel recorded force on the cylinder and the second recorded wave height. The event marker was utilized through an external jack to record the frequency of the imposed motion and to establish the motion/force phase relationship.

B. TEST PROCEDURE

1. System Selection and Optimization

The first step in the procedure was to select one of two sets of holding and balancing arms to provide the desired $\bar{d}/\bar{a}$ ratio and to mount them on the center drum. Wooden shims were available in 1/2 inch thickness which allowed placement of either cylinder at two or three radii from the wave channel bottom. Once a set of holding and balancing arms was chosen, the dimensionless parameter $\bar{d}/\bar{a}$ varied with water depth.

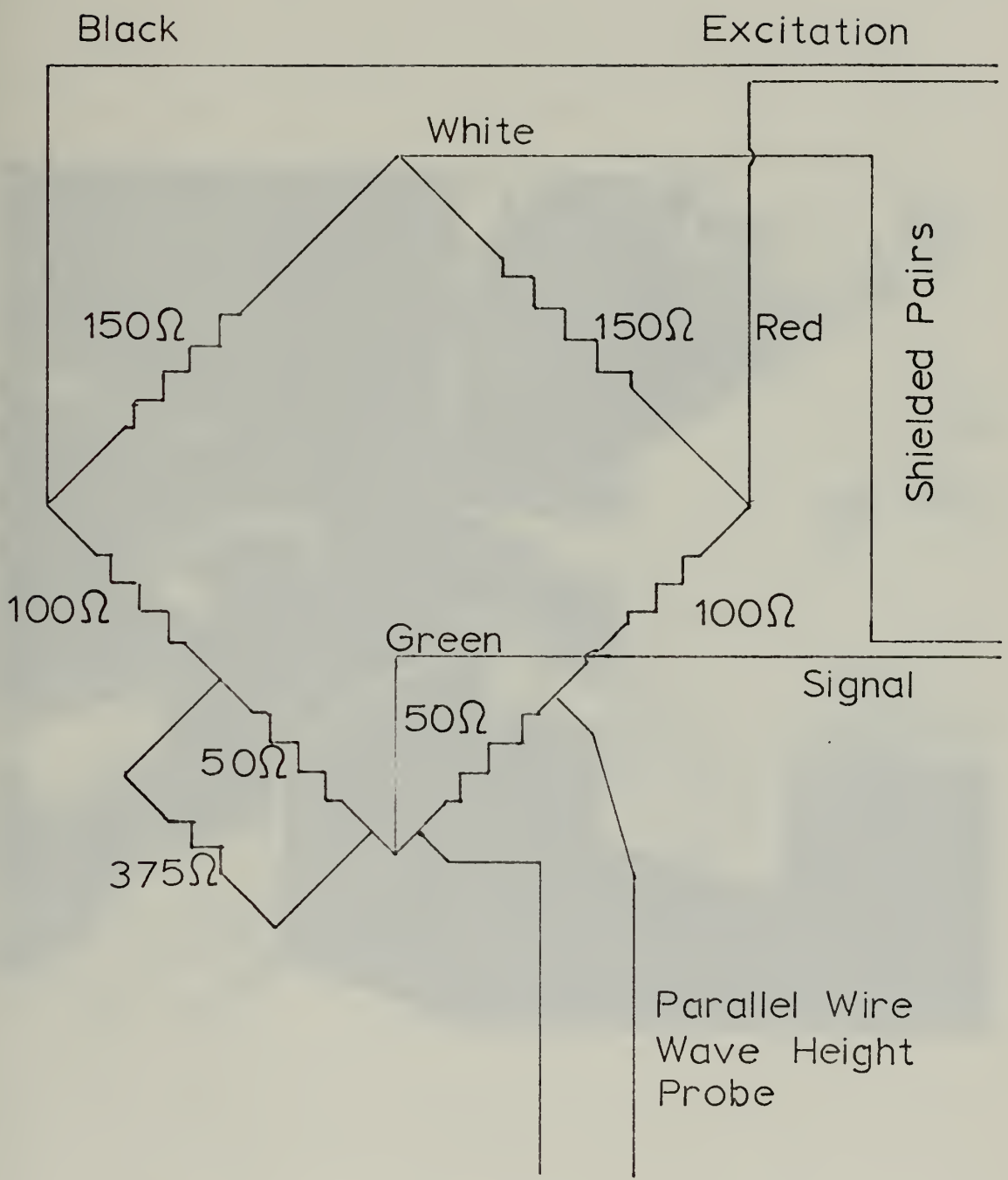

FIGURE 12. WAVE HEIGHT GAUGE BRIDGE SCHEMATIC

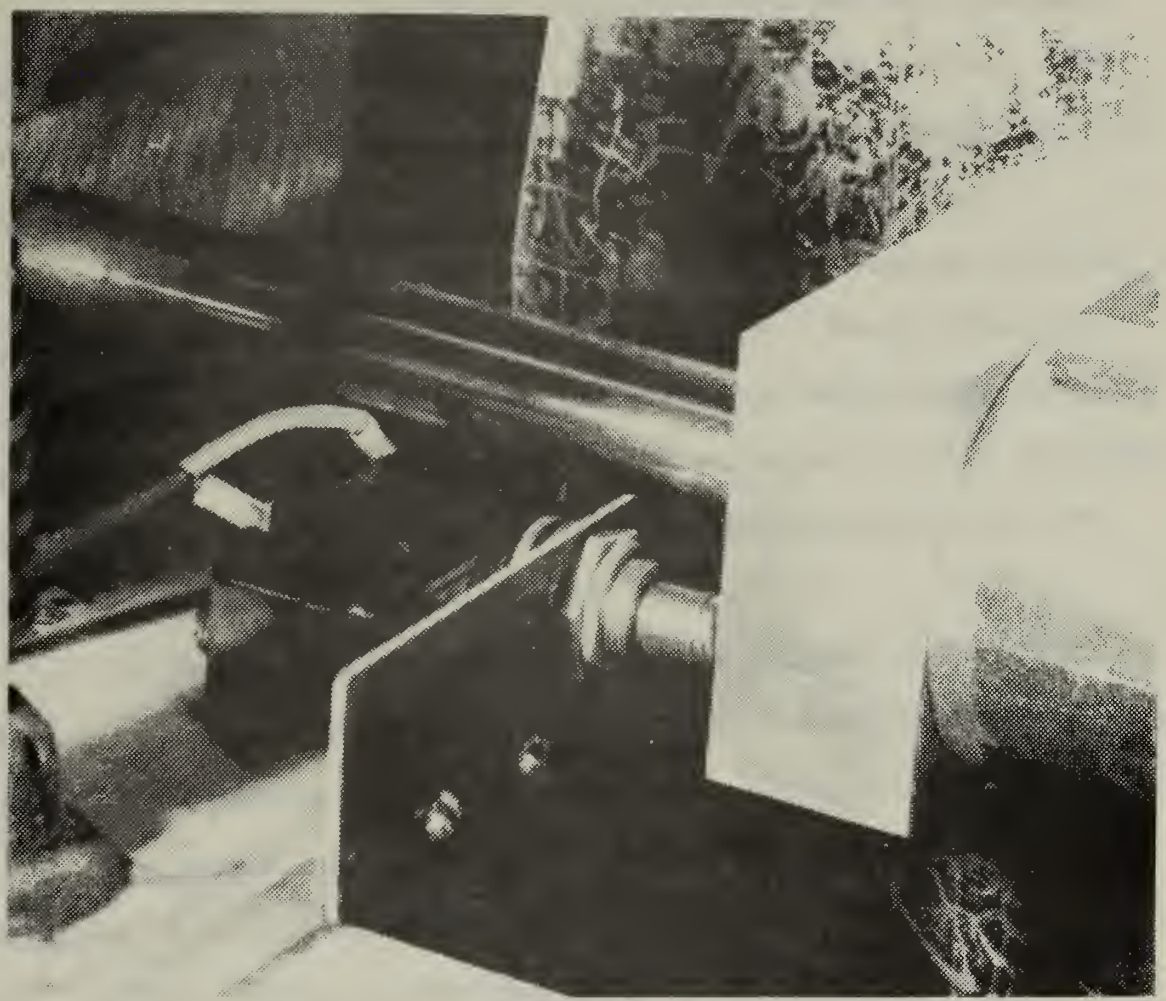

FIGURE 13. R.P.M. SWITCH

The next step was to decide whether it was desired to examine the lower or higher range of dimensionless frequency parameters. The larger six inch OD plexiglass cylinder was used for the lower range of frequency parameters because its larger displaced volume produced forces which were more readily measurable. However, at higher frequencies the larger cylinder resulted in natural to forcing frequency ratios too close to 1.0 to give valid results. The larger six inch OD cylinder was, therefore, used at the lower motor speed range of from 22 to about 100 rpm. The smaller four inch OD aluminum cylinder was used at upper speed range of from about 100 to 180 rpm.

Once the combination of holding and balancing arms and cylinder was chosen, the cylinder was attached to the arms. The cylinder was sealed and the cylinder holding and balancing jig was balanced using the adjustable counter balancing weight. After balancing, the jig was placed in position on the carriage and the carriage properly positioned and clamped to the top of the wave channel.

The desired stroke was adjusted at the variable speed transmission face plate. The stroke was maintained at a value of 0.1 $\bar{a}$ to insure that separated flow did not occur.

The channel was filled and data runs conducted at water levels which were 2, 3, and 4 cylinder radii above the cylinder center.

After the wave channel was filled to the desired level, the Wheatstone bridges were balanced and a test run was made through the frequency range to determine the optimum attenuation settings, chart speed, and beam position to obtain the most readable results. At this time the entire assembly was "plucked" to determine the natural to forced frequency ratio. If the value of this ratio was less than five, the beam was adjusted to the position which provided the stiffest beam.

2. System Calibration

a. Force Calibration

After balancing the bridge and selecting the appropriate attenuator setting, a piece of light weight plastic line was tied loosely around the center of the test cylinder and bent around a low friction pulley located at the top of the channel, 100 inches from the test cylinder. Weights were hung from the line and the resulting deflection on the recording paper recorded. The angle which the string made with the horizontal was accurately measured and the resultant horizontal component of force determined. The strain gauge bridge was calibrated in this manner in both directions separately. The results were plotted accurately to insure linearity and to be used to interpret data. The calibration of the strain gauge bridge was checked frequently between data runs. See Appendix A for a typical force calibration plot.

b. Wave Height Calibration

After balancing the bridge and selecting the proper attenuator setting the wave height gauge was calibrated by utilizing the block stand to immerse and withdraw the wire a known distance. The following procedure was used. The gauge was raised 1/2 inch simulating a decrease in water level, then lowered 1/2 inch below the null, simulating an increase in water level. Then, the gauge was raised one inch and lowered one inch, etc. This procedure closely simulated the actual passage of a wave profile with crests and troughs. Resulting deflections on the recording paper were accordingly recorded and the results accurately plotted to insure linearity and to be later used to interpret data. The calibration of the wave height meter was checked frequently between data runs. See Appendix A for a typical wave height calibration plot.

c. Event Marker Calibration

The ability of the event marker to record the frequency of the imposed motion and the phase angle was dependent upon the accuracy of the chart speed. The accuracy of the chart speed was checked against the internal timer of the recorder. No discrepancy was found.

3. Data Run

After system selection and optimization was accomplished and system calibration completed, a data run was conducted. The system is shown in Figure (14). The data run was commenced with the variable speed transmission set at the lower value of rpm corresponding to the lower value of the range of desired frequency parameters. The inductance motor and recorder were turned on simultaneously. The recorder was allowed to run until the channel recording wave height indicated a steady state had been reached. The recorder was then secured and the transmission adjusted to the next rpm value corresponding to the next desired frequency parameter. The meter was then sevured and the wave action in the channel allowed to subside before the next data point was recorded. This procedure was repeated until the desired range of frequency parameters had been covered.

At the end of each data run, a calibration check was conducted on both the wave height gauge and strain gauge bridge.

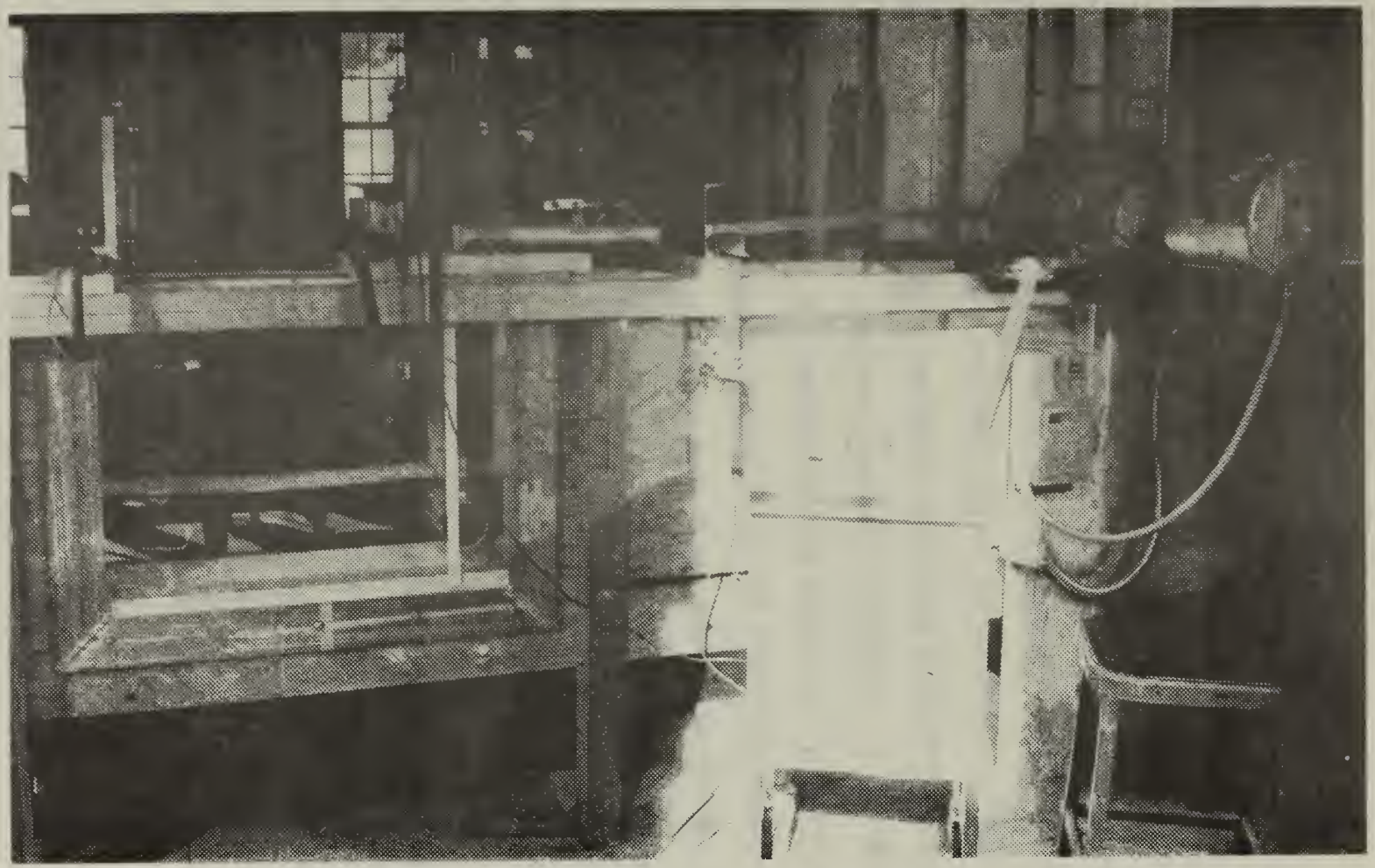

FIGURE 14. ASSEMBLED SYSTEM

IV. EXPERIMENTAL RESULTS

As shown in Equation (3) in THEORETICAL CONSIDERATIONS, the force coefficient can be represented as a function of relative water depth, relative depth of submergence, relative amplitude, and a dimensionless frequency parameter. The dynamic forces on the object may be expressed as the sum of two components, one component in phase with acceleration and one component in phase with the velocity of the cylinder. The coefficient of the acceleration component represents added mass and the coefficient of the velocity component represents damping. It follows that these two coefficients are determinable by measuring the force on the cylinder and the phase angle between force and acceleration.

Additionally, if a control volume were drawn around the system, it could be shown through a consideration of conservation of energy that the wave energy flux out must equal the energy associated with damping if viscous effects are disregarded. Therefore, wave height is directly related to the degree of damping.

Accordingly, a program was designed to measure forces, phase angles between force and acceleration, and wave heights within a range of independent dimensionless variable limited by time and equipment available.

Twelve data sets were taken at six variations of relative water depth (d) and relative depth of submergence (h). The six variations were: $d = 2.0$, $h = 4.0$; $d = 2.0$, $h = 5.0$; $d = 3.0$, $h = 5.0$; $d = 3.0$, $h = 6.0$; $d = 4.0$, $h = 6.0$; $d = 4.0$, $h = 7.0$. All data sets were taken at a relative displacement (x) of 0.1. The range of dimensionless frequency parameters (ν) for each run was from 0.04 to 1.7. The low frequency half

of each run was conducted with a six inch OD plexiglass cylinder and the high frequency half with a four inch OD aluminum cylinder. An overlap between high frequency and low frequency parameters of approximately 0.36 was provided near mid-range.

A. EXAMPLE STRIP CHART READ-OUT

An example of a strip chart read-out is presented in Figure (15). For this particular run $\bar{a} = 3$, $\bar{d} = 6.0$, $\bar{h} = 12.0$. The values read from the chart for this data point were wave height (WH) = 0.088 inches, force = 0.3525 pounds, period = 143 millimeters, phase angle (PA) = 8 millimeters, and chart speed = 100 millimeters per second.

The wave profiles are nearly sinusoidal. The natural frequency of the entire mechanism is seen superimposed upon the force profile. It is apparent that the natural frequency is considerably greater than the forcing frequency. Difficulty was encountered in reading phase angle from the chart. A chart speed of 100 millimeters per second was required to resolve phase angle. Because of the superposition of natural frequency upon the force profile, it was necessary to "fair" the force profile to properly read phase angle. The result of reading phase angle in this manner led to inaccuracies, especially at lower frequencies where forces were small and resulting force profiles relatively flat.

B. DATA REDUCTION

A computer program was written to reduce experimental data. The program is presented in Appendix B with tabulated results for each data point.

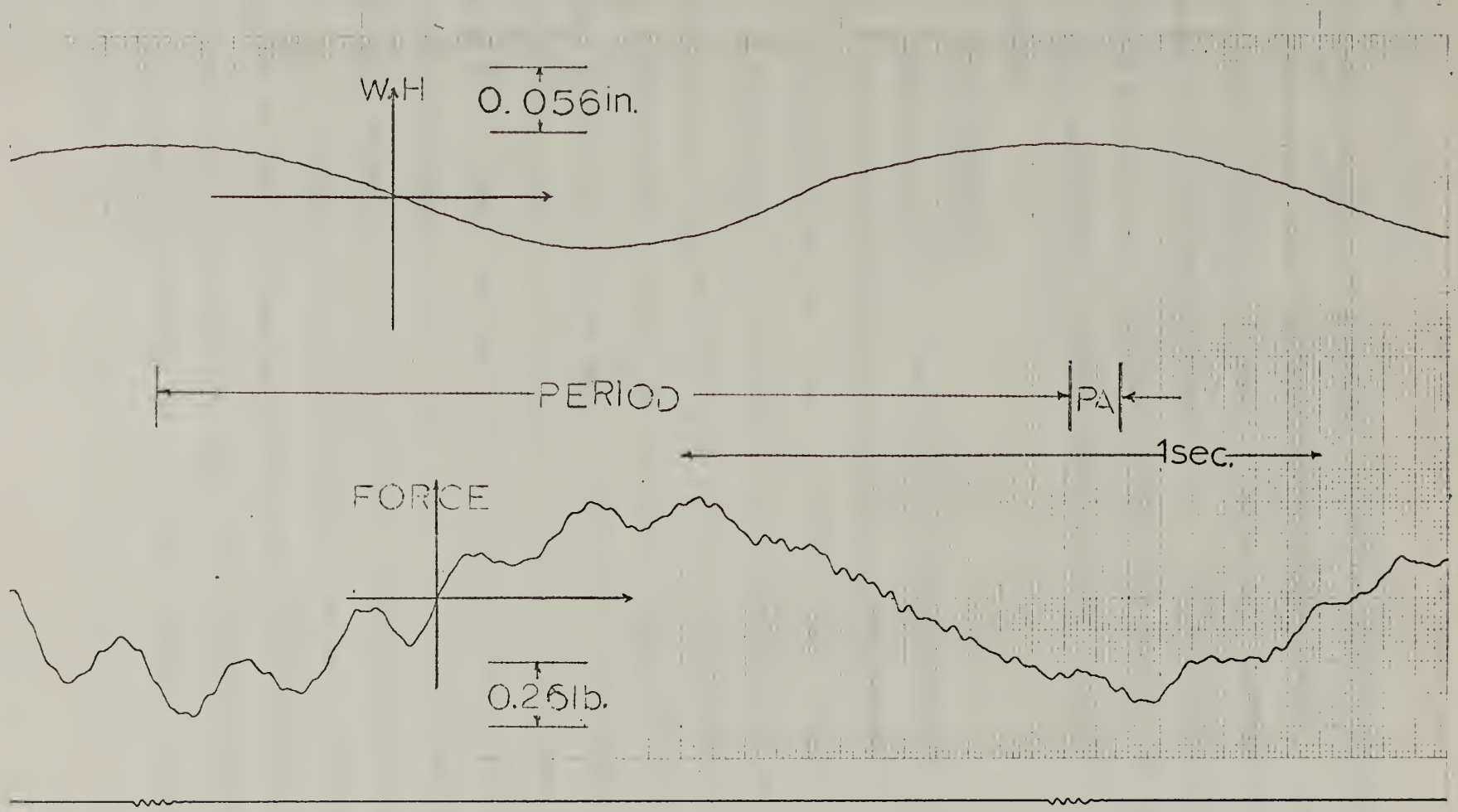

FIGURE 15. EXAMPLE STRIP CHART READ-OUT

C. PRESENTATION OF RESULTS

Experimental results are presented in graphical form in Figures (16-23). For each combination of the dimensionless parameters d and h, a graph of force coefficient, phase angle, and wave height ratio was drawn to exhibit dependence upon the frequency parameter. In a few cases theoretical curves, provided by Garrison in an unpublished paper, were drawn in for comparison. Smooth curves were "faired" in cases where Garrison's theoretical data was not complete.

1. Force Coefficient

Despite the scatter in the values of force coefficient, results compared favorably with Garrison's theoretical curves, except at the lower end of the frequency spectrum. See Figures (18), (22), and (23).

A consideration of the boundary value problem associated with the problem resulted in the conclusion that the free surface boundary would act as a solid boundary at very low frequencies and as a constant pressure boundary at very high frequencies. It follows that force coefficient as a function of frequency should approach a constant value asymtotically at both the high frequency and low frequency end of the data range and vary in a continuous manner between. Also, since the constant pressure boundary at the high frequency end tends to eliminate pressure differences in the fluid, it follows that the constant asymtotic value at the higher frequency end should be lower. Further, it follows that as the relative proximity of the free surface increases, the effect should be more pronounced. The results as presented in Figures (16, 18, 20-23) indicate that these effects were observed.

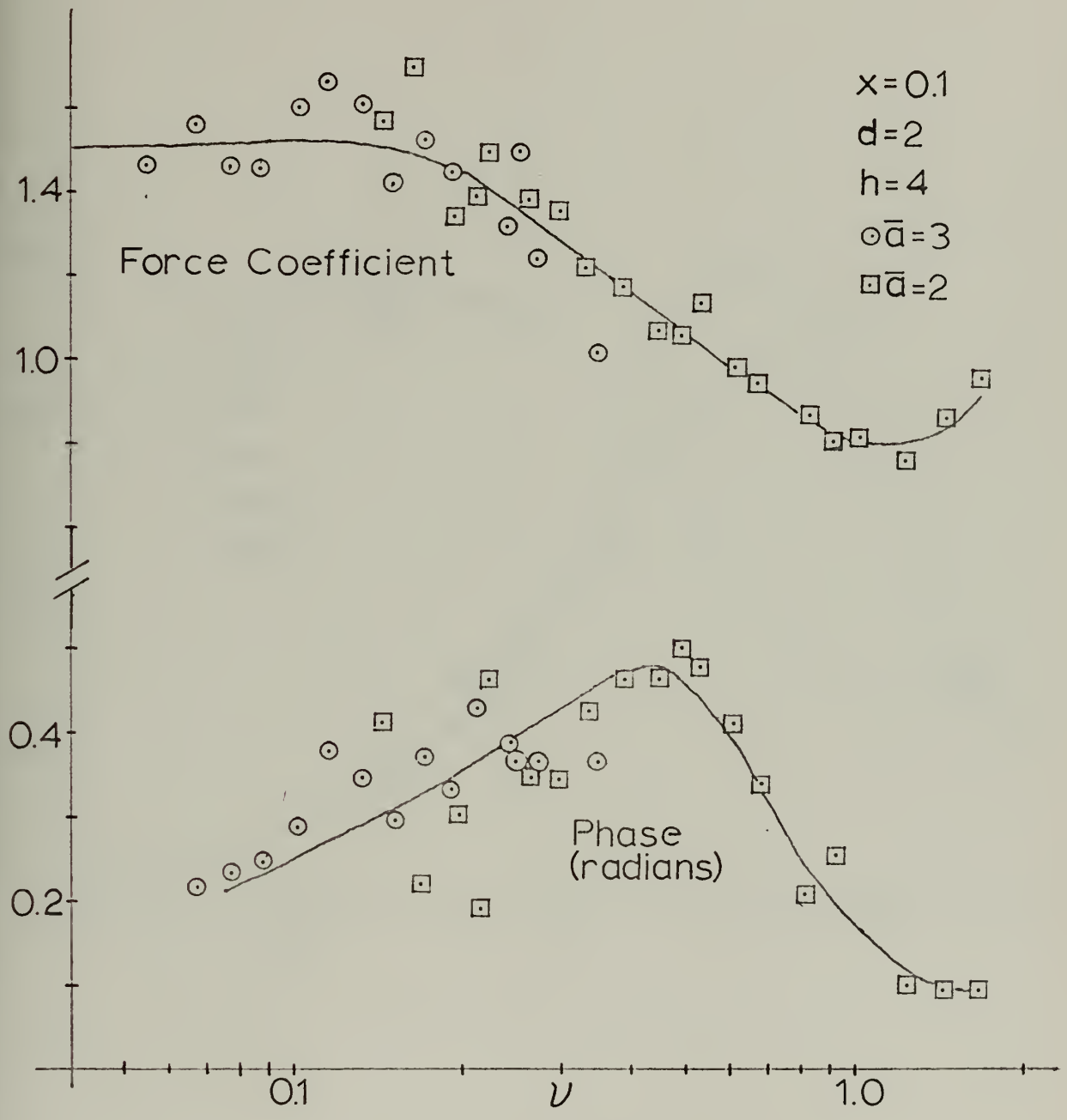

FIGURE 16. FORCE COEFFICIENTS AND PHASE ANGLE

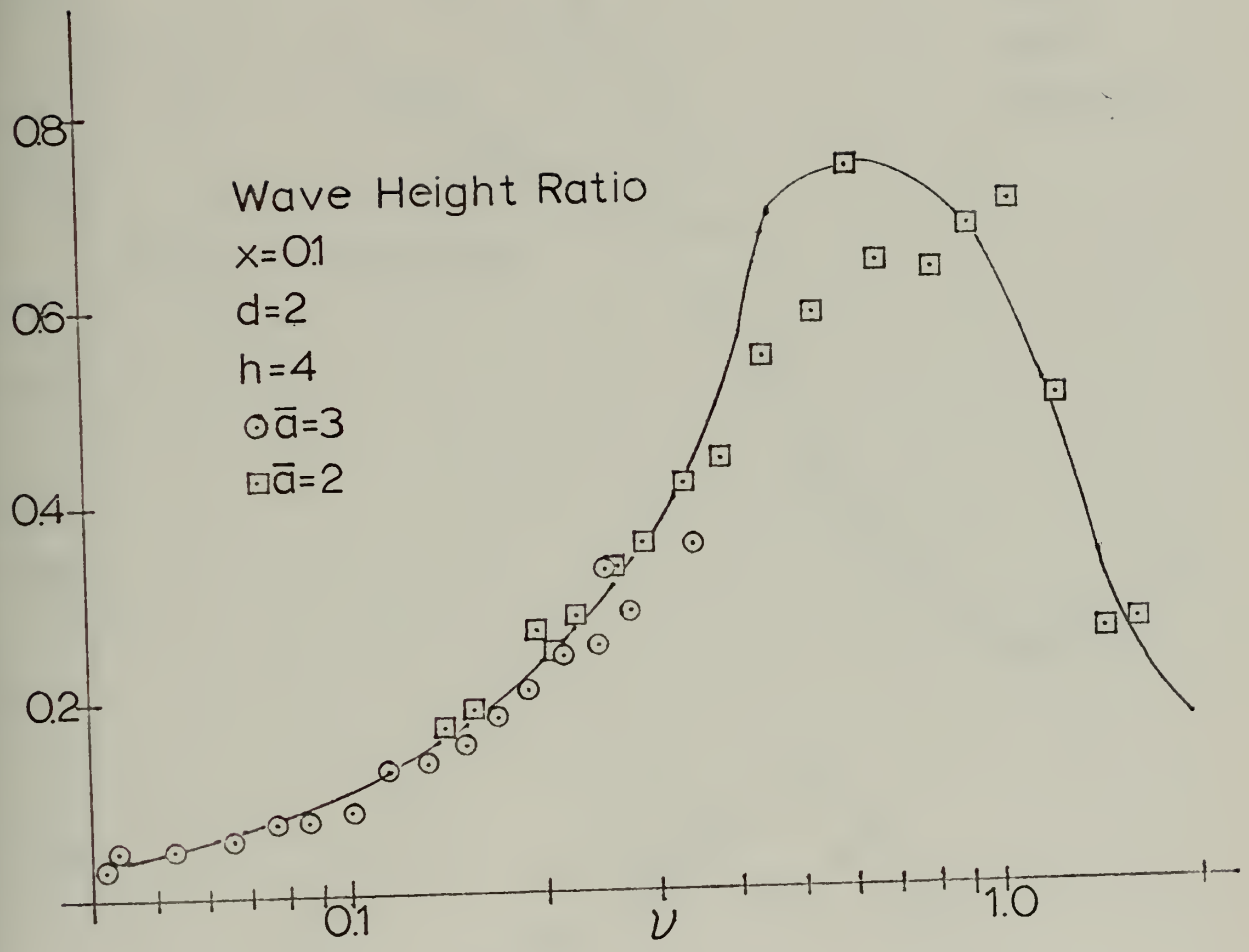

FIGURE 17. WAVE HEIGHT RATIO

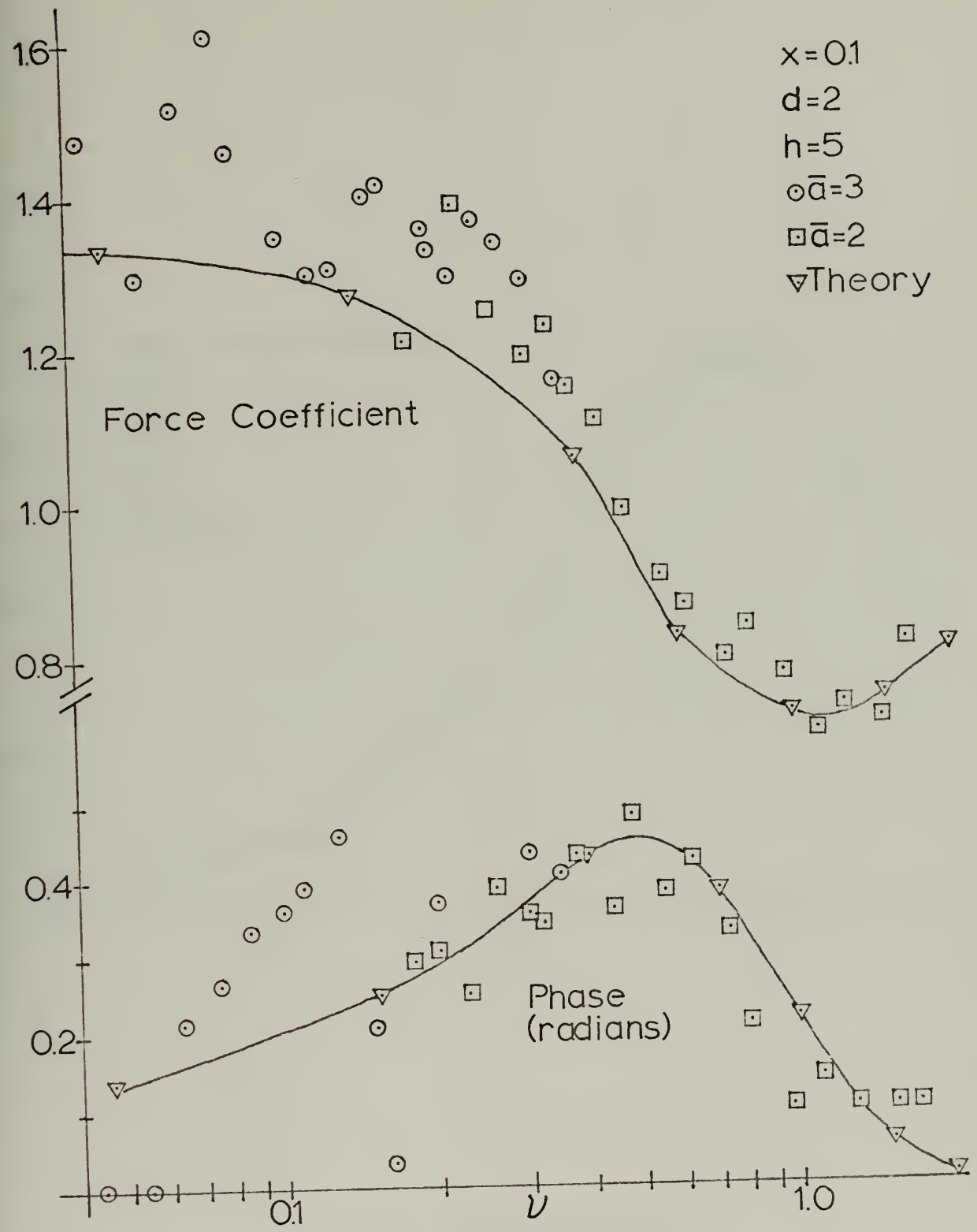

FIGURE 18. FORCE COEFFICIENTS AND PHASE ANGLE

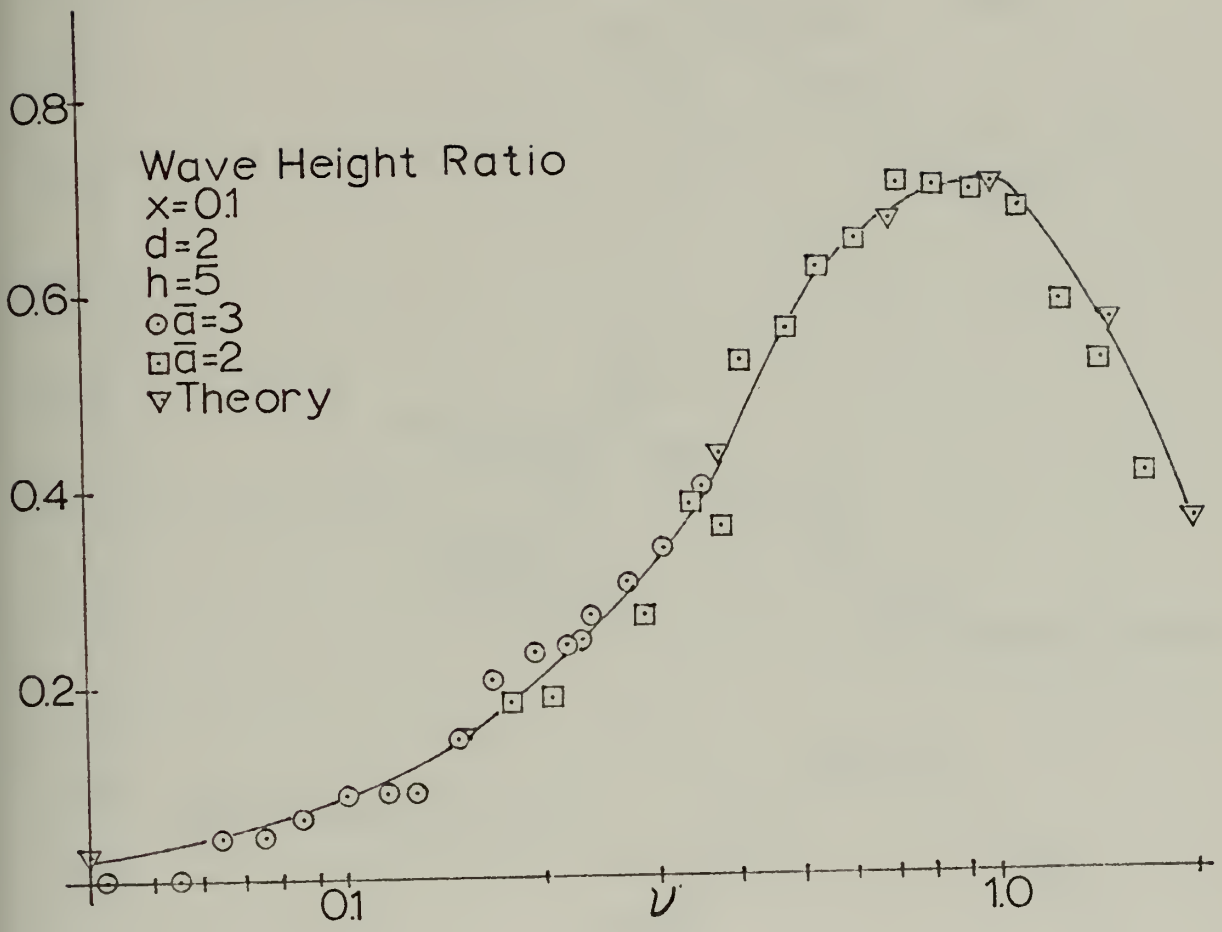

FIGURE 19. WAVE HEIGHT RATIO

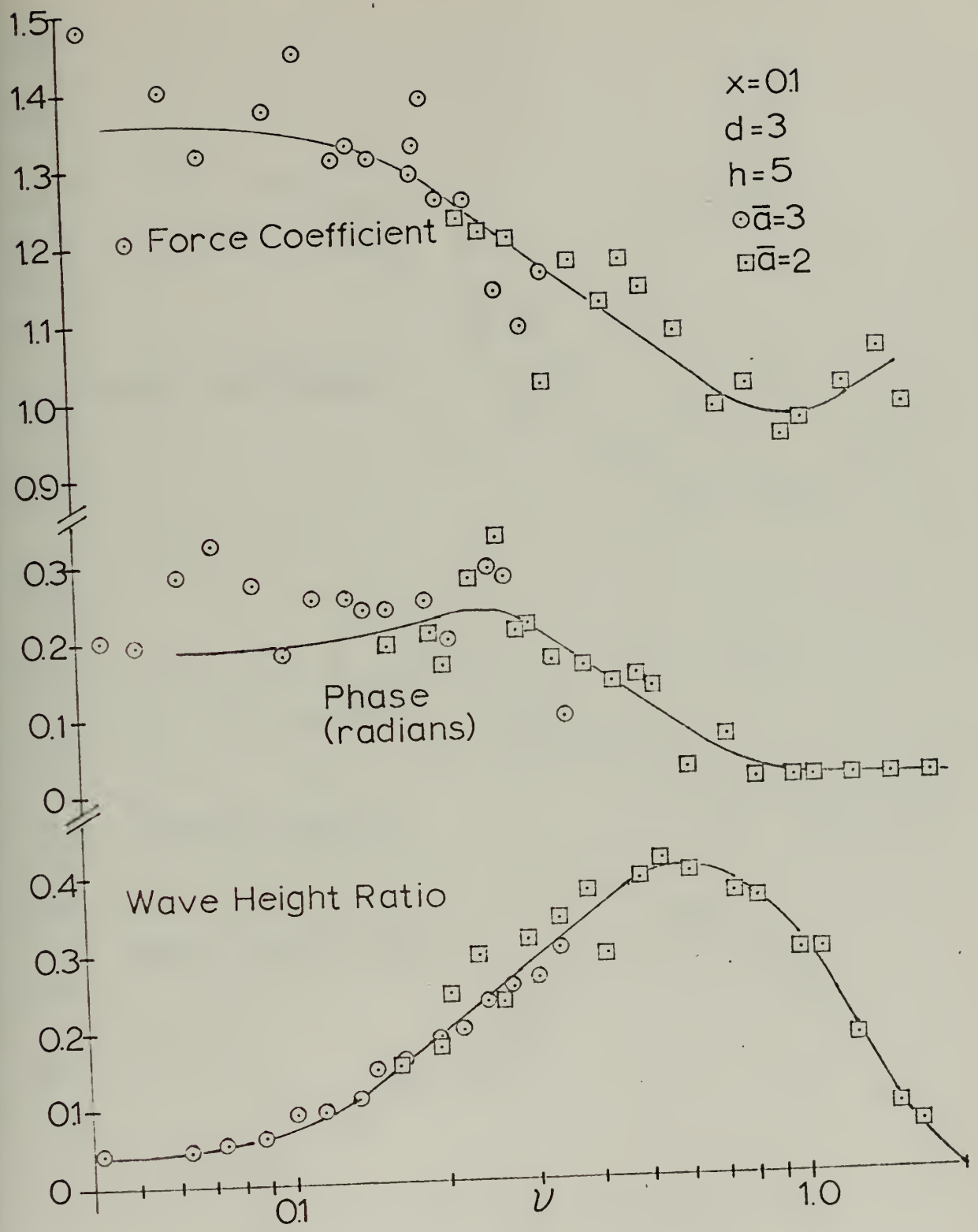

FIGURE 20. FORCE COEFFICIENTS, PHASE ANGLE, AND WAVE HEIGHT RATIO

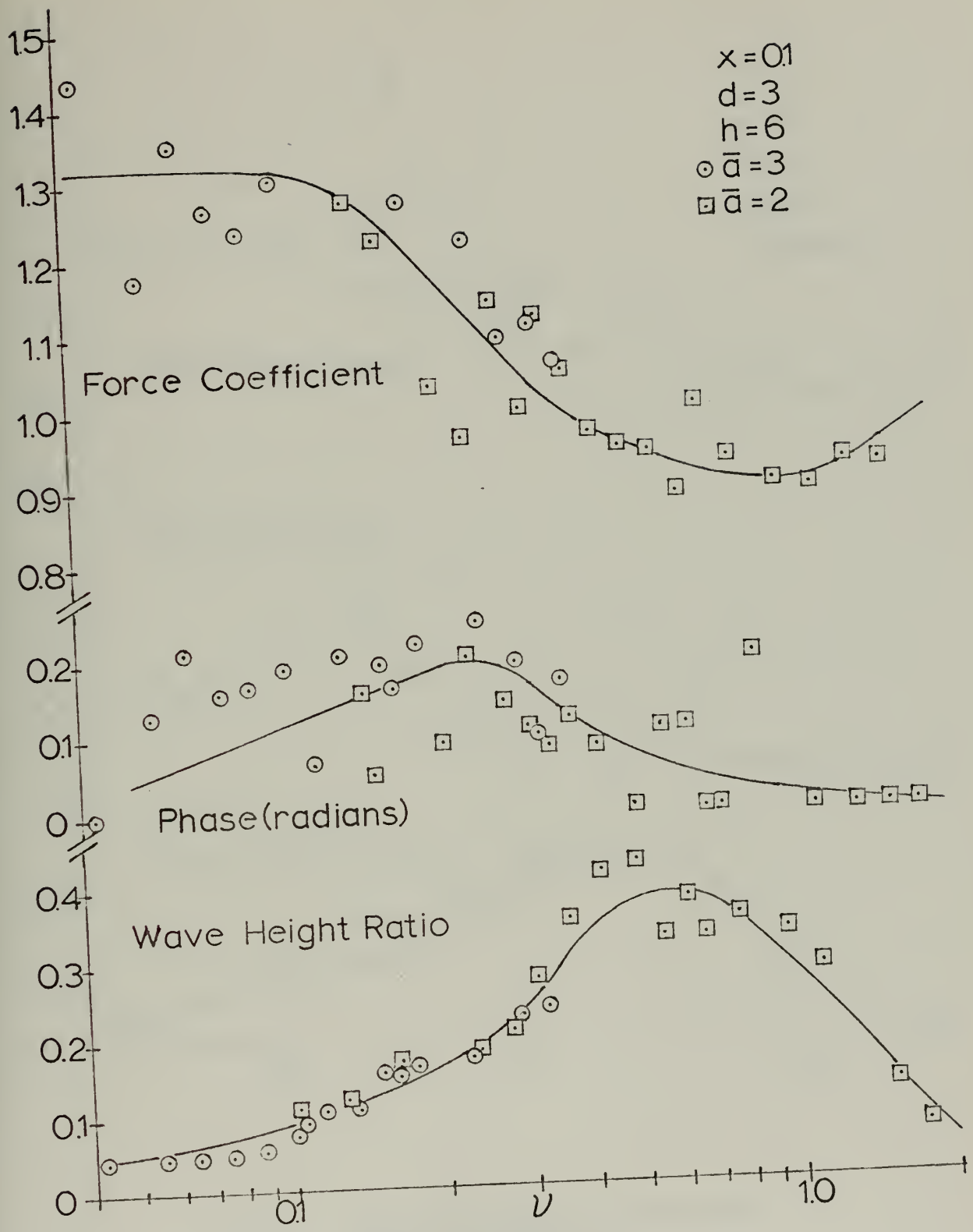

FIGURE 21. FORCE COEFFICIENTS, PHASE ANGLE, AND WAVE HEIGHT RATIO

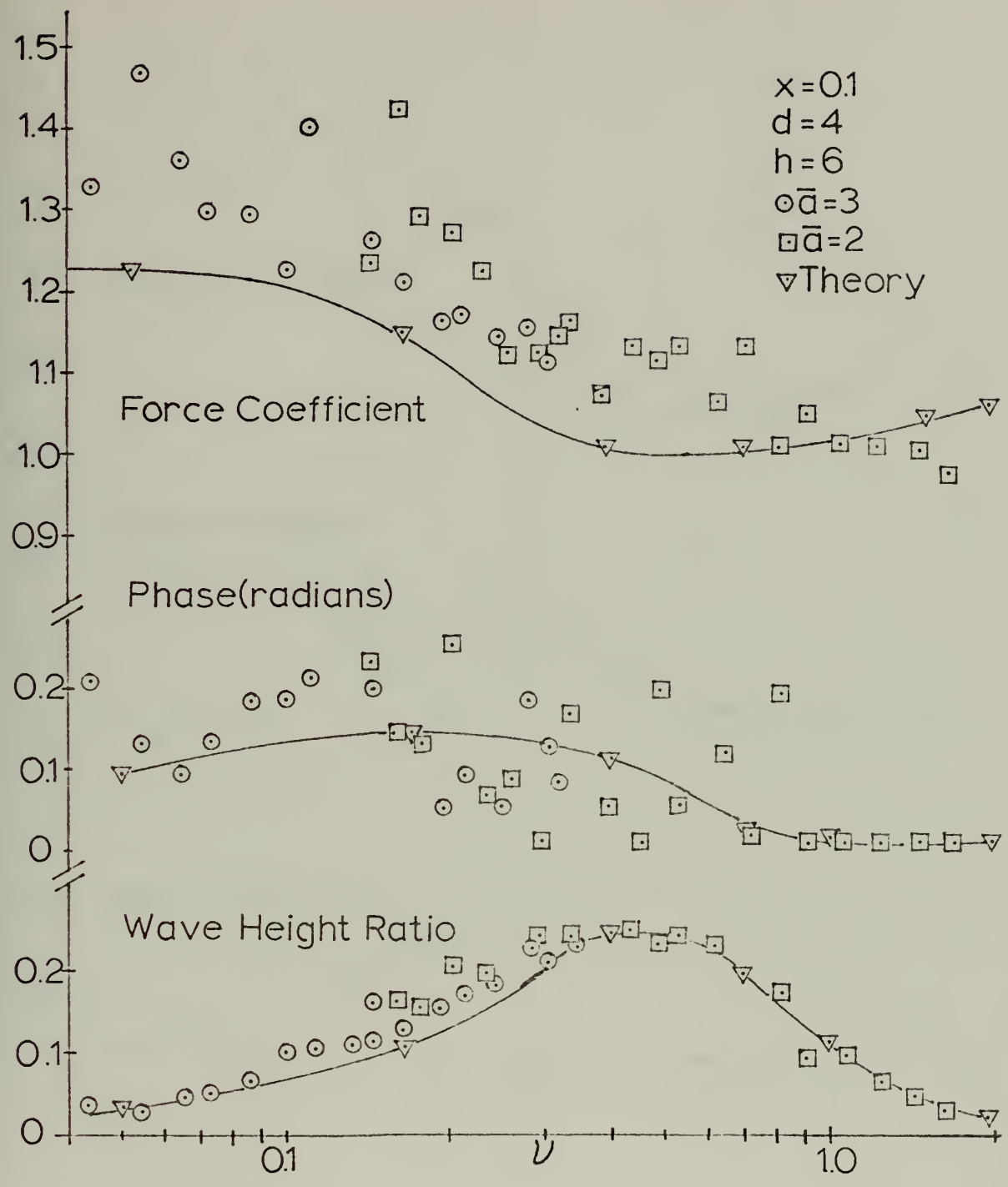

FIGURE 22. FORCE COEFFICIENTS, PHASE ANGLE, AND WAVE HEIGHT PATIO

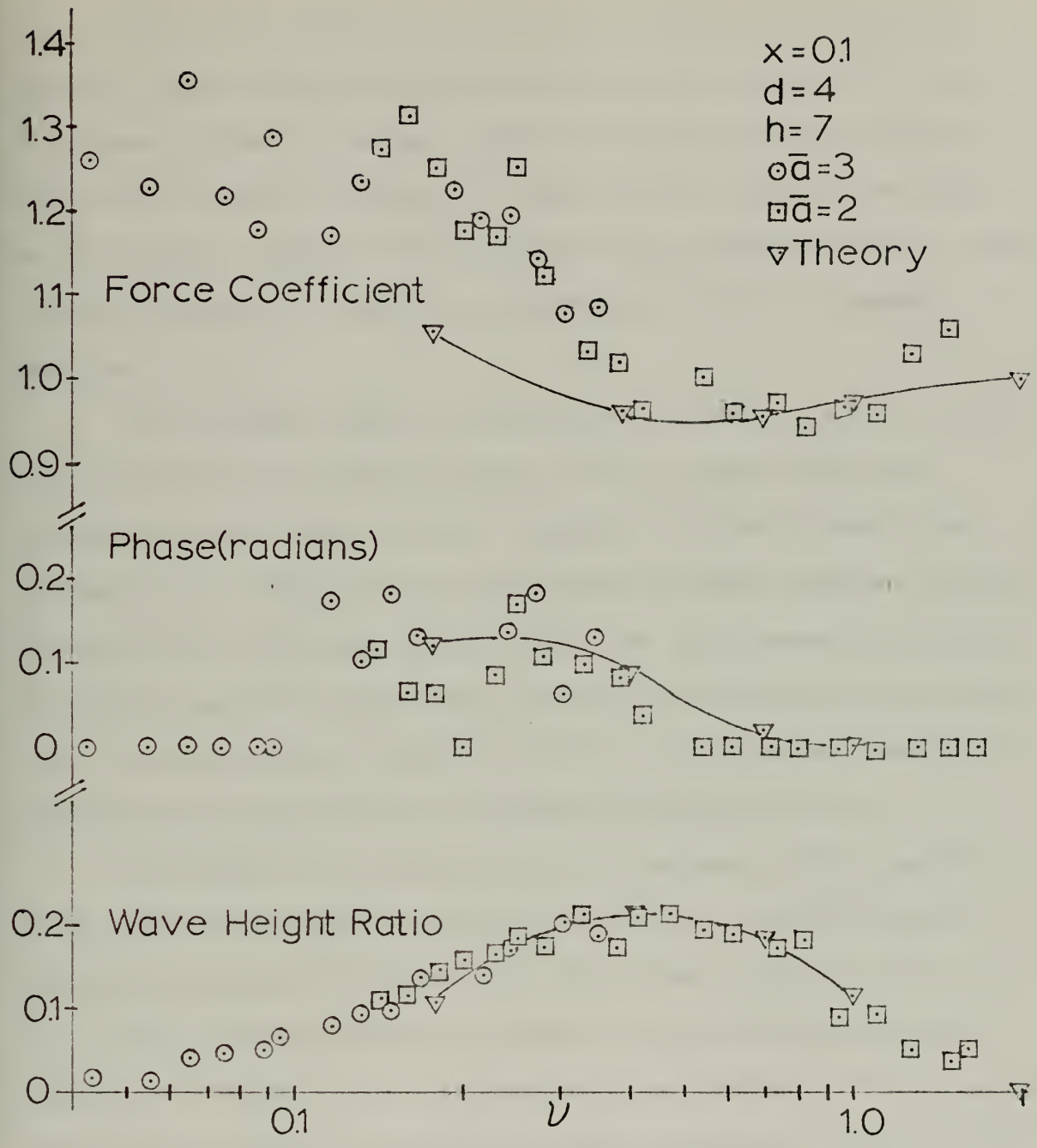

FIGURE 23. FORCE COEFFICIENTS, PHASE ANGLE, AND WAVE HEIGHT RATIO

Figure (16) indicates that for d = 2.0 and h = 4.0 the lower frequency value of force coefficient was approximately 1.5. The range of frequency parameters did not extend to high enough values to determine the high frequency asymptote. Theoretical data was not available for this figure, therefore a mean line was drawn through the data. Force coefficient appeared to reach a minimum value of 0.8 at a frequency parameter of 1.15.

At the greatest depth of submergence, (d = 4.0, h = 6.0), Figure (22) indicates that the lower frequency value of force coefficient decreased to 1.38. Again, the high frequency asymptotic behavior was undeterminable. Garrison's theoretical data at these parameters indicate that the force coefficient is still lower than experimentally indicated throughout almost the entire range of frequency parameters by as much as 10%. The minimum value of force coefficient at this larger submergence depth was approximately 1.0 at a frequency parameter of 1.10.

The effect of the proximity of the impermeable bottom surface can be observed by comparing Figures (16) and (18). During these two data runs, relative submergence depth (d) was held constant at d = 2.0 while relative water depth (h) was varied. Similar comparisons were made at d = 3.0 and d = 4.0. In each case, the proximity of the impermeable bottom surface appeared to increase the force coefficient over the entire range tested.

It may be noted that the scatter in values of force coefficient was greatest at the low frequency end of the range of frequency coefficients. This was attributable to the nature of the error in force measurement. It was observed that although the error in force measurement could be assumed relatively constant, the magnitude of force measured at values

of $\nu < 0.1$ was very small, often smaller by an order of magnitude than the magnitude of the force measured at values of $\mu > 0.1$. It follows that with constant absolute error, the relative error can be expected to be an order of magnitude larger. In every case scatter was reduced at higher frequencies where forces were larger. Also in the area where overlap occurred between high and low frequency data sets, the results appear consistant and repeatable. It was observed that for values of

0.1, almost all of the data was consistant within 10%.

2. Phase Angle and Wave Height

Values of phase angle and wave height compared favorably with Garrison's theoretical curves. See Figures (18), (19), (22), and (23). As stated earlier, the added mass coefficient is determinable if the force coefficient and the phase angle are known. Further, a theoretical consideration resulted in the conclusion that added mass coefficient may be computed by multiplying force coefficient by the cosine of the phase angle. The balance of the force coefficient is attributable to damping and consequently, the damping coefficient may be obtained by multiplying the force coefficient by the sine of the phase angle. Also, as stated earlier, from a consideration of conservation of energy, wave height may be used as a measure of the degree of damping.

The value of phase angle and wave height at the extremes of the frequency spectrum was predicted by intuitively assuming that at very low frequencies the force and motion would be in phase, and at very high frequencies damping would be non-existant. It was predicted that phase angle and wave height would be non-existant where force coefficient approached a constant value asymptotically. It followed that force coefficient and added mass coefficient would be synonymous near the

asymptotes. The effect of a free surface was predicted to be more predominant at lower values of relative depth of submergence. The results as presented in Figures (16-23) indicate that these effects were observed.

Figure (16) indicates that for d = 2.0 and h = 4.0 the phase angle was zero for frequency parameters greater than 1.5. The lower frequency data was not complete for phase. However, Figure (17) indicates that wave height was zero for frequency parameters less than 0.4. Figures (16) and (17) show phase and wave height reached maximum values of 0.48 radians and 0.74 inches respectively.

At the greatest depth of submergence, Figure (22) indicates that for d = 4.0 and h = 6.0 the phase angle was zero for frequency parameters greater than 0.9. Again, the phase angle did not vanish at lower frequencies but wave height vanished for frequency parameters less than 0.4. Maximum values were about 0.15 radians and 0.24 inches for phase angle and waveheight respectively. As predicted, values were considerably less than those observed at a smaller relative submerged depth.

The effect of the proximity of the impermeable bottom on the phase angle can be observed by comparing Figures (16) and (18). The maximum value appears to be reduced and shifted slightly to the left. A similar reduction and shift to the left were observed in the maximum value of waveheight between Figures (17) and (19).

Again, despite the scatter in the values of phase angle, the results compare favorably with Garrison's theoretical curves. In cases where theoretical curves were not available the trend in data was "faired in".

All the remarks above pertaining to measuring small magnitude forces with constant absolute error apply also to the measurement of phase. Accurate measurement of phase angle was especially difficult in the lower frequency ranges where force profiles were flat. The exact point where the force changed direction was difficult to determine accurately. Consequently, more scatter was observed in the phase data. It was for this reason that no attempt was made to plot the added mass dependency upon frequency parameter. Rather, the resulting sets of force coefficient data and phase data were considered separately. Added mass is presented in tabular form as computer program output in Appendix B.

V. CONCLUSIONS

An experimental study of the added mass of a right circular cylinder under a free surface has been conducted. From the results of this study, the following conclusions were drawn.

1. Results agreed within 10% with theoretical results proposed by Garrison in an unpublished paper.

2. The relative proximity of a free surface induced a pronounced variation in added mass coefficient from the classical value of 1.0.

3. When the cylinder was oscillated at very low frequencies and at at very high frequencies, the value of the added mass coefficient was constant. This constant value was larger at a low frequency than at high frequency due to the fact that at low frequency the free surface acts as a rigid boundary.

4. The proximity of an impermeable bottom surface had the effect on the value of the added mass coefficient of raising its magnitude at all frequencies.

5. A phase angle between induced force on the cylinder and the acceleration experienced by the cylinder was observed to be a function of frequency. This phase angle vanished at high and at low frequencies.

6. The proximity of either a free surface or an impermeable bottom surface had an effect of raising the magnitude of the maximum value of phase angle and shifting the occurrence of this maximum to a lower frequency value.

7. When the cylinder was oscillated, induced waves were observed. Wave height was a function of frequency of oscillation. Induced waves vanished at low and at high frequencies.

8. The proximity of either a free surface or an impermeable bottom surface had the effect of raising the magnitude of the maximum value of wave height and shifting the occurrence of this maximum to a lower frequency value.

APPENDIX A

FIGURE 24. TYPICAL FORCE CALIBRATION CURVE

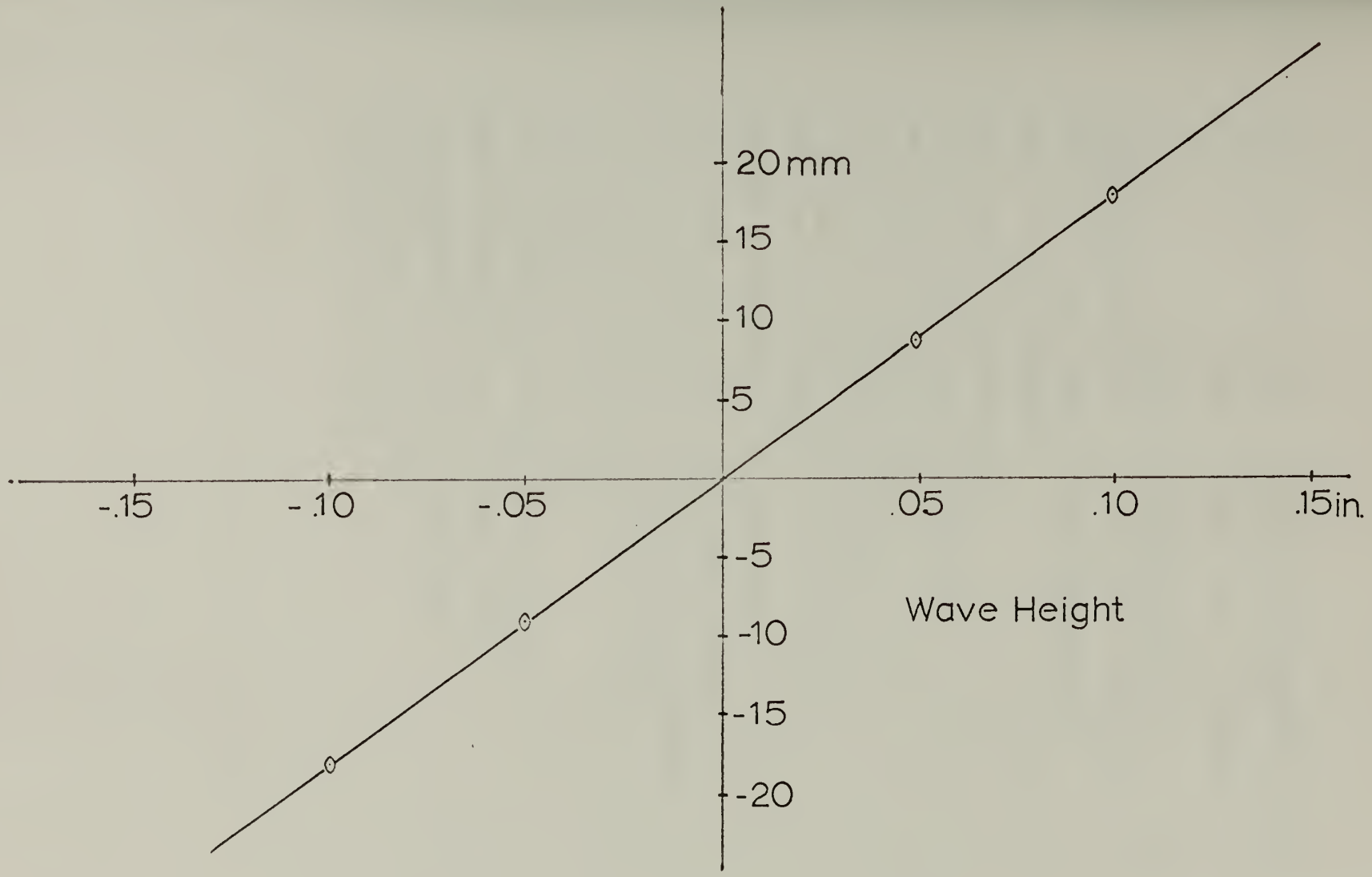

FIGURE 25. TYPICAL WAVE HEIGHT CALIBRATION CURVE

APPENDIX B COMPUTER PRORAM

```
C     THIS PROGAM WAS USED TO REDUCE EXPERIMENTAL DATA.

C     DEFINITION OF PARAMETERS USED ARE AS FOLLOWS:

C     T=PERIOD OF FORCING FUNCTION(SECONDS)
C     SIGMA=ANGULAR FREQUENCY OF FORCING FUNCTION
C     (RADIANS/SECOND)
C     G=GRAVITATIONAL CONSTANT(FEET/SECOND**2)
C     HB=WATER DEPTH(INCHES)
C     AB=CYLINDER RADIUS(INCHES)
C     RHO=WATER DENSITY(SLUGS/FEET**3)
C     LB=CYLINDER LENGTH(INCHES)
C     DB=DEPTH OF SUBMERGENCE(INCHES)
C     WH=TROUGH TO CREST WAVE HEIGHT(INCHES)
C     F=MAXIMUM FORCE(POUNDS)
C     XB=HALF AMPLITUDE OF MOTION(INCHES)
C     TMM=PERIOD READ FROM CHART(MILLIMETERS)
C     PMM=PHASE SHIFT READ FROM CHART(MILLIMETERS)
C     CSPEED=CHART SPEED(MILLIMETERS/SECOND)
C     PHASE=PHASE SHIFT(RADIANS)
C     NCARD=NUMBER OF DATA CARDS
C     ANU=DIMENSIONLESS FREQUENCY PARAMETER
C     WHR=DIMENSIONLESS WAVE HEIGHT RATIO
C     FC=DIMENSIONLESS FORCE COEFFICIENT
C     AM=ADDED MASS COEFFICIENT
C     DN=DAMPING COEFFICIENT
```

```
   10 FORMAT(4F10.4,I10)
   15 FORMAT('1',20X,'AB=',F8.4,5X,'DB=',F8.4,5X,'HB=',F8.4,
     15X,'XB=',F8.4,5X,'NCARD=',I3)
   20 FORMAT('0',20X,'X=',F8.4,5X,'D=',F8.4,5X,'H=',F8.4)
   25 FORMAT(5F10.4)
   65 FORMAT('0',7X,'SIGMA',10X,'F',7X,'CSPEED',8X,'ANU',10X
     1,'FC',6X,'PHASE',10X,'AM',8X,'DN',9X,'WHR')
   80 FORMAT('0',9F12.4)

C      ASSIGN SPECIFIC VALUES TO CONSTANTS TO BE LATER USED
       G=32.174
       RHO=62.4/G
C      THIS PROGRAM WAS DESIGNED TO HANDLE TWELVE DATA SETS
       DO 300 K=1,12
C      READ IN PARAMETERS WHICH CHARACTERIZE DATA SET
       READ(5,10) AB,DB,HB,XB,NCARD
C      PRINT PARAMETERS FOR LATER REFERENCE
       WRITE(6,15) AB,DB,HB,XB,NCARD
C      COMPUTE VALUES OF DIMENSIONLESS PARAMETERS
       D=DB/AB
       H=HB/AB
       X=XB/AB
C      PRINT DIMENSIONLESS PARAMETERS
       WRITE(6,20) X,D,H
C      PRINT COLUMN HEADINGS FOR INPUT / OUTPUT PARAMETERS
       WRITE(6,65)
C      COMMENCE DATA REDUCTION
       DO 200 I=1,NCARD
C      READ INPUT PARAMETERS
       READ(5,25) F,WH,TMM,PMM,CSPEED
C      COMPUTE PERIOD OF FORCING FUNCTION
       T=TMM/CSPEED
C      COMPUTE PHASE ANGLE
       PHASE=2.*3.14159*PMM/TMM
C      COMPUTE ANGULAR FREQUENCY OF FORCING FUNCTION
       SIGMA=2.*3.14159/T
C      COMPUTE DIMENSIONLESS FREQUENCY PARAMETER
       ANU=SIGMA**2*AB/(G*12)
```

```
C       COMPUTE WAVE HEIGHT RATIO
        WHR=(WH/2.)/XB
C       COMPUTE VOLUME OF CYLINDER
        VOL=3.14159*AB**2*1.25/144.
C       COMPUTE FORCE COEFFICIENT
        FC=F/(RHO*VOL*SIGMA**2*XB/12.)
C       COMPUTE ADDED MASS COEFFICIENT
        AM=FC*COS(PHASE)
C       COMPUTE DAMPING COEFFICIENT
        DN=FC*SIN(PHASE)
C       COMPUTATION COMPLETE. PRINT VALUE OF PARAMETERS AT
C       THIS POINT AND RETURN TO BEGINNING OF LOOP TO LOOK
C       AT THE NEXT DATA POINT IN THIS SET.
        WRITE(6,80) SIGMA,F,CSPEED,ANU,FC,PHASE,AM,DN,WHR
  200   CONTINUE
C       GO TO NEXT DATA SET.
  300   CONTINUE
        STOP
        END
```

APPENDIX B (CONTINUED)

DATA RUN NUMBER 1

AB=3.0 DB=6.0 HB=12.0 XB=0.32 NCARD=17 X=0.1 D=2.0 H=4.0

SIGMA	F	ANU	FC	PHASE	AM	DN	WHR
2.37	0.09	0.04	1.33	0.35	1.24	0.46	0.05
2.32	0.11	0.04	1.67	0.34	1.57	0.57	0.02
2.64	0.13	0.05	1.46	0.26	1.41	0.38	0.05
2.92	0.17	0.06	1.56	0.21	1.53	0.34	0.05
3.14	0.18	0.07	1.47	0.23	1.43	0.34	0.07
3.35	0.21	0.08	1.47	0.25	1.42	0.36	0.07
3.61	0.26	0.10	1.60	0.28	1.53	0.45	0.08
3.85	0.31	0.11	1.68	0.38	1.55	0.63	0.10
4.10	0.34	0.13	1.62	0.34	1.52	0.55	0.13
4.39	0.35	0.15	1.43	0.29	1.37	0.42	0.13
4.68	0.42	0.17	1.52	0.37	1.41	0.55	0.17
4.94	0.45	0.19	1.46	0.33	1.38	0.48	0.20
5.28	0.49	0.21	1.39	0.43	1.26	0.58	0.23
5.61	0.53	0.24	1.32	0.39	1.22	0.50	0.25
5.92	0.56	0.27	1.25	0.37	1.17	0.45	0.29
5.76	0.64	0.25	1.51	0.37	1.41	0.55	0.33
6.75	0.60	0.35	1.04	0.37	0.97	0.37	0.35

APPENDIX B (CONTINUED)

DATA RUN NUMBER 2

AB=2.0 DB=4.0 HB=8.0 XB=0.20 NCARD=20 X=0.1 D=2.0 H=4.0

SIGMA	F	ANU	FC	PHASE	AM	DN	WHR
5.23	0.15	0.14	1.57	0.41	1.44	0.64	0.17
5.66	0.19	0.16	1.70	0.22	1.65	0.38	0.19
6.16	0.18	0.19	1.32	0.30	1.26	0.40	0.27
6.41	0.20	0.21	1.39	0.19	1.36	0.26	0.24
6.61	0.23	0.22	1.50	0.46	1.34	0.67	0.28
7.14	0.23	0.26	1.28	0.35	1.20	0.45	0.33
7.57	0.26	0.29	1.26	0.35	1.18	0.44	0.35
8.05	0.28	0.33	1.22	0.42	1.11	0.50	0.41
8.60	0.31	0.38	1.18	0.47	1.05	0.54	0.44
9.24	0.33	0.44	1.09	0.46	0.98	0.48	0.54
9.66	0.36	0.48	1.09	0.50	0.95	0.53	0.87
10.13	0.41	0.53	1.11	0.48	0.98	0.51	0.59
10.83	0.41	0.60	0.97	0.83	0.65	0.72	0.74
11.42	0.45	0.67	0.96	0.34	0.90	0.32	0.64
12.56	0.50	0.81	0.88	0.21	0.86	0.19	0.63
13.36	0.51	0.92	0.80	0.26	0.77	0.21	0.67
13.96	0.57	1.00	0.82	0.00	0.82	0.00	0.72
15.41	0.66	1.23	0.77	0.00	0.77	0.00	0.50
16.75	0.90	1.45	0.89	0.00	0.89	0.00	0.26
17.95	1.02	1.66	0.88	0.00	0.88	0.00	0.27

APPENDIX B (CONTINUED)

DATA RUN NUMBER 3

AB=3.0 DB=9.0 HB=15.0 XB=0.32 NCARD=16 X=0.1 D=3.0 H=5.0

SIGMA	F	ANU	FC	PHASE	AM	DN	WHR
2.32	0.10	0.04	1.49	0.20	1.46	0.30	0.04
2.61	0.10	0.05	1.20	0.19	1.18	0.23	0.28
2.85	0.14	0.06	1.40	0.28	1.34	0.39	0.04
3.09	0.16	0.07	1.31	0.32	1.24	0.42	0.05
3.37	0.22	0.08	1.55	0.27	1.40	0.41	0.06
3.59	0.22	0.10	1.37	0.17	1.35	0.24	0.09
3.83	0.27	0.11	1.44	0.24	1.40	0.35	0.09
4.16	0.28	0.13	1.30	0.24	1.26	0.32	0.10
4.33	0.31	0.14	1.32	0.23	1.28	0.31	0.14
4.65	0.36	0.16	1.30	0.23	1.27	0.30	0.15
4.98	0.40	0.19	1.28	0.24	1.24	0.31	0.19
5.28	0.44	0.21	1.24	0.19	1.21	0.24	0.19
5.61	0.50	0.24	1.25	0.28	1.20	0.34	0.23
5.92	0.50	0.27	1.13	0.26	1.09	0.29	0.25
6.28	0.54	0.30	1.08	0.20	1.06	0.21	0.26
6.61	0.64	0.33	1.15	0.09	1.14	0.11	0.30

APPENDIX B (CONTINUED)

DATA RUN NUMBER 4

AB=2.0 DB=6.0 HB=10.0 XB=0.20 NCARD=19 X=0.1 D=3.0 H=5.0

SIGMA	F	ANU	FC	PHASE	AM	DN	WHR
5.56	0.10	0.16	0.90	0.19	0.88	0.17	0.15
6.16	0.18	0.19	1.32	0.20	1.29	0.26	0.17
6.28	0.19	0.20	1.38	0.15	1.36	0.21	0.24
6.75	0.20	0.23	1.22	0.27	1.17	0.32	0.29
7.14	0.22	0.26	1.20	0.32	1.14	0.38	0.22
7.48	0.24	0.28	1.19	0.20	1.17	0.24	0.31
8.05	0.24	0.33	1.05	0.16	1.04	0.16	0.33
8.60	0.31	0.38	1.16	0.15	1.15	0.17	0.37
8.97	0.32	0.41	1.10	0.13	1.09	0.14	0.29
9.66	0.39	0.48	1.16	0.14	1.15	0.16	0.38
10.13	0.41	0.53	1.12	0.12	1.12	0.14	0.41
10.83	0.45	0.60	1.07	0.02	1.07	0.02	0.39
11.85	0.49	0.72	0.97	0.05	0.97	0.05	0.37
12.56	0.56	0.81	0.99	0.00	0.99	0.00	0.36
13.65	0.62	0.96	0.92	0.00	0.92	0.00	0.29
14.44	0.71	1.08	0.95	0.00	0.95	0.00	0.29
15.70	0.88	1.27	0.99	0.00	0.99	0.00	0.18
16.98	1.08	1.49	1.04	0.00	1.04	0.00	0.08
17.95	1.12	1.66	0.97	0.00	0.97	0.00	0.07

APPENDIX B (CONTINUED)

DATA RUN NUMBER 5

AB=3.0 DB=12.0 HB=18.0 XB=0.32 NCARD=16 X=0.1 D=4.0 H=6.0

SIGMA	F	ANU	FC	PHASE	AM	DN	WHR
2.37	0.09	0.04	1.33	0.20	1.30	0.27	0.03
2.64	0.13	0.05	1.46	0.13	1.45	0.19	0.02
2.89	0.14	0.06	1.36	0.09	1.35	0.12	0.04
3.06	0.15	0.07	1.29	0.13	1.28	0.17	0.05
3.36	0.18	0.08	1.29	0.18	1.26	0.23	0.06
3.63	0.20	0.10	1.22	0.18	1.20	0.22	0.10
3.85	0.26	0.11	1.40	0.21	1.37	0.29	0.10
4.13	0.35	0.13	1.61	0.20	1.57	0.33	0.10
4.33	0.30	0.14	1.25	0.19	1.23	0.24	0.11
4.65	0.33	0.16	1.21	0.34	1.14	0.41	0.13
5.02	0.37	0.19	1.16	0.05	1.16	0.05	0.15
5.23	0.41	0.21	1.17	0.09	1.17	0.10	0.16
5.66	0.46	0.24	1.14	0.05	1.14	0.06	0.18
6.04	0.51	0.28	1.11	0.18	1.09	0.20	0.23
6.28	0.55	0.30	1.10	0.12	1.09	0.13	0.20
6.61	0.63	0.33	1.14	0.08	1.13	0.09	0.23

APPENDIX B (CONTINUED)

DATA RUN NUMBER 6

AB=2.0 DB=8.0 HB=12.0 XB=0.20 NCARD=20 X=0.1 D=4.0 H=6.0

SIGMA	F	ANU	FC	PHASE	AM	DN	WHR
5.32	0.12	0.14	1.23	0.23	1.19	0.29	0.16
5.61	0.16	0.16	1.42	0.14	1.40	0.19	0.16
5.87	0.16	0.17	1.29	0.13	1.28	0.17	0.15
6.28	0.18	0.20	1.27	0.25	1.23	0.31	0.20
6.75	0.20	0.23	1.22	0.06	1.22	0.08	0.19
7.05	0.20	0.25	1.12	0.08	1.11	0.09	0.28
7.57	0.23	0.29	1.12	0.00	1.12	0.00	0.24
8.05	0.27	0.33	1.16	0.16	1.24	0.18	0.24
8.60	0.28	0.38	1.07	0.04	1.07	0.04	0.20
9.17	0.33	0.43	1.11	0.00	1.11	0.00	0.24
9.66	0.38	0.48	1.15	0.19	1.12	0.22	0.23
10.13	0.43	0.53	1.16	0.05	1.16	0.05	0.24
11.02	0.46	0.62	1.06	0.11	1.06	0.11	0.22
11.74	0.56	0.71	1.13	0.00	1.13	0.00	0.31
12.56	0.61	0.81	1.07	0.18	1.06	0.20	1.17
13.22	0.72	0.90	1.14	0.00	1.14	0.00	0.09
14.44	0.82	1.08	1.09	0.00	1.09	0.00	0.09
15.51	0.92	1.24	1.06	0.00	1.06	0.00	0.06
16.75	1.02	1.45	1.01	0.00	1.01	0.00	0.04
17.95	1.12	1.66	0.97	0.00	0.97	0.00	0.02

APPENDIX B (CONTINUED)

DATA RUN NUMBER 7

AB=3.0 DB=6.0 HB=15.0 XB=0.29 NCARD=16 X=0.1 D=2.0 H=5.0

SIGMA	F	ANU	FC	PHASE	AM	DN	WHR
2.32	0.09	0.04	1.46	0.00	1.48	0.00	0.00
2.64	0.10	0.05	1.30	0.00	1.30	0.00	0.00
2.87	0.14	0.06	1.52	0.21	1.49	0.32	0.04
3.10	0.17	0.07	1.60	0.27	1.54	0.43	0.04
3.35	0.18	0.08	1.46	0.33	1.38	0.48	0.06
3.61	0.20	0.10	1.35	0.36	1.26	0.47	0.08
3.86	0.22	0.11	1.30	0.38	1.20	0.48	0.08
4.08	0.25	0.12	1.31	0.45	1.18	0.58	0.08
4.39	0.31	0.15	1.40	0.21	1.36	0.30	0.15
4.65	0.35	0.16	1.41	0.03	1.41	0.04	0.20
5.02	0.39	0.19	1.36	0.27	1.31	0.37	0.23
5.32	0.42	0.22	1.30	0.89	0.81	1.01	0.23
5.63	0.50	0.24	1.36	0.95	0.78	1.11	0.26
5.92	0.54	0.27	1.34	0.97	0.73	1.11	0.30
6.28	0.58	0.30	1.29	0.43	1.17	0.55	0.34
6.75	0.61	0.35	1.16	0.43	1.07	0.45	0.40

APPENDIX B (CONTINUED)

DATA RUN NUMBER 8

AB=2.0 DB=4.0 HB=10.0 XB=0.19 NCARD=18 X=0.1 D=2.0 H=5.0

SIGMA	F	ANU	FC	PHASE	AM	DN	WHR
5.98	0.15	0.18	1.21	0.29	1.16	0.35	0.18
6.28	0.18	0.20	1.32	0.31	1.26	0.40	0.18
6.61	0.21	0.22	1.39	0.24	1.35	0.34	0.24
7.14	0.22	0.26	1.25	0.32	1.19	0.39	0.29
7.66	0.24	0.30	1.18	0.30	1.13	0.35	0.33
8.05	0.27	0.33	1.23	0.28	1.18	0.34	0.38
8.49	0.28	0.37	1.14	0.38	1.06	0.42	0.46
8.97	0.31	0.41	1.11	0.35	1.04	0.39	0.53
9.66	0.32	0.48	0.99	0.48	0.88	0.46	0.56
10.30	0.33	0.54	0.91	0.38	0.85	0.34	0.62
10.92	0.36	0.61	0.87	0.41	0.80	0.35	0.64
11.85	0.39	0.72	0.80	0.32	0.76	0.25	0.71
12.44	0.45	0.80	0.84	0.21	0.82	0.18	0.70
13.51	0.49	0.94	0.78	0.10	0.77	0.07	0.70
14.61	0.51	1.10	0.70	0.14	0.69	0.10	0.68
15.70	0.63	1.27	0.74	0.00	0.74	0.00	0.58
16.75	0.72	1.45	0.74	0.00	0.74	0.00	0.52
17.95	0.91	1.66	0.82	0.00	0.82	0.00	0.41

APPENDIX B (CONTINUED)

DATA RUN NUMBER 9

AB=3.0 DB=9.0 HB=18.0 XB=0.29 NCARD=16 X=0.1 D=3.0 H=6.0

SIGMA	F	ANU	FC	PHASE	AM	DN	WHR
2.32	0.09	0.04	1.44	0.00	1.44	0.00	0.04
2.65	0.09	0.05	1.17	0.13	1.16	0.15	0.04
2.88	0.13	0.06	1.35	0.21	1.32	0.29	0.04
3.10	0.14	0.07	1.26	0.15	1.24	0.19	0.04
3.35	0.16	0.08	1.23	0.16	1.22	0.20	0.05
3.61	0.19	0.10	1.30	0.18	1.28	0.23	0.07
3.63	0.27	0.10	1.79	0.10	1.78	0.19	0.09
3.85	0.28	0.11	1.63	0.05	1.63	0.09	0.10
4.09	0.28	0.13	1.49	0.21	1.45	0.31	0.10
4.39	0.32	0.15	1.44	0.19	1.41	0.28	0.15
4.58	0.33	0.16	1.39	0.16	1.37	0.22	0.15
4.88	0.35	0.18	1.27	0.22	1.24	0.27	0.16
5.58	0.44	0.24	1.22	0.25	1.18	0.30	0.16
6.10	0.46	0.28	1.08	0.19	1.06	0.21	0.22
6.41	0.52	0.31	1.11	0.09	1.10	0.10	0.23
6.75	0.55	0.35	1.05	0.16	1.04	0.17	0.27

APPENDIX B (CONTINUED)

DATA RUN NUMBER 10

AB=2.0 DB=6.0 HB=12.0 XB=0.19 NCARD=19 X=0.1 D=3.0 H=6.0

SIGMA	F	ANU	FC	PHASE	AM	DN	WHR
5.23	0.12	0.14	1.27	0.15	1.25	0.19	0.12
5.56	0.13	0.16	1.22	0.05	1.22	0.06	0.16
6.28	0.14	0.20	1.03	0.09	1.02	0.09	0.14
6.75	0.15	0.23	0.95	0.20	0.93	0.19	0.18
7.22	0.20	0.27	1.14	0.14	1.13	0.16	0.20
7.70	0.20	0.30	1.00	0.11	0.99	0.11	0.27
8.05	0.25	0.33	1.12	0.08	1.11	0.09	0.28
8.37	0.26	0.36	1.07	0.12	1.06	0.13	0.35
8.97	0.27	0.41	0.97	0.08	0.97	0.08	0.40
9.66	0.30	0.48	0.94	0.00	0.94	0.00	0.42
10.30	0.34	0.54	0.94	0.10	0.94	0.09	0.32
10.83	0.36	0.60	0.89	0.10	0.88	0.09	0.37
11.42	0.45	0.67	1.00	0.00	1.00	0.00	0.32
12.20	0.48	0.77	0.93	0.00	0.93	0.00	0.35
13.51	0.57	0.94	0.90	0.20	0.88	0.18	0.33
14.61	0.65	1.10	0.89	0.00	0.89	0.00	0.28
15.90	0.81	1.31	0.93	0.00	0.93	0.00	0.19
17.21	0.94	1.53	0.92	0.00	0.92	0.00	0.12
18.47	1.13	1.76	0.96	0.00	0.96	0.00	0.06

APPENDIX B (CONTINUED)

DATA RUN NUMBER 11

AB=3.0 DB=12.0 HB=21.0 XB=0.29 NCARD=16 X=0.1 D=4.0 H=7.0

SIGMA	F	ANU	FC	PHASE	AM	DN	WHR
2.34	0.08	0.04	1.26	0.00	1.26	0.00	0.01
2.65	0.10	0.05	1.22	0.00	1.22	0.00	0.01
2.88	0.13	0.06	1.35	0.00	1.35	0.00	0.04
3.10	0.13	0.07	1.21	0.00	1.21	0.00	0.05
3.35	0.15	0.08	1.18	0.00	1.18	0.00	0.05
3.43	0.17	0.09	1.29	0.00	1.29	0.00	0.06
3.90	0.20	0.11	1.17	0.17	1.15	0.20	0.07
4.13	0.24	0.13	1.23	0.10	1.22	0.12	0.09
4.39	0.34	0.15	1.53	0.18	1.50	0.28	0.09
4.65	0.35	0.16	1.40	0.13	1.39	0.19	0.13
4.98	0.35	0.19	1.22	0.39	1.12	0.47	0.13
5.32	0.38	0.22	1.18	0.33	1.12	0.38	0.13
5.61	0.43	0.24	1.19	0.14	1.18	0.16	0.16
5.98	0.47	0.27	1.14	0.19	1.11	0.22	0.16
6.28	0.49	0.30	1.07	0.06	1.07	0.06	0.20
6.75	0.57	0.35	1.08	0.13	1.07	0.14	0.18

APPENDIX B (CONTINUED)

DATA RUN NUMBER 12

AB=2.0 DB=8.0 HB=14.0 XB=0.19 NCARD=20 X=0.1 D=4.0 H=7.0

SIGMA	F	ANU	FC	PHASE	AM	DN	WHR
5.23	0.12	0.14	1.27	0.11	1.26	0.14	0.10
5.56	0.14	0.16	1.31	0.06	1.31	0.09	0.11
5.89	0.15	0.18	1.25	0.05	1.25	0.07	0.14
6.28	0.16	0.20	1.17	0.00	1.17	0.00	0.15
6.68	0.18	0.23	0.17	0.08	1.16	0.10	0.16
6.98	0.21	0.25	1.25	0.17	1.23	0.21	0.19
7.39	0.21	0.28	1.11	0.11	1.11	0.12	0.17
8.05	0.23	0.33	1.03	0.10	1.02	0.10	0.21
8.60	0.26	0.38	1.02	0.08	1.01	0.08	0.17
9.04	0.27	0.42	0.96	0.04	0.95	0.04	0.20
9.52	0.36	0.46	1.17	0.23	1.13	0.27	0.21
10.21	0.36	0.54	1.00	0.00	1.00	0.00	0.18
10.83	0.39	0.60	0.96	0.00	0.96	0.00	0.18
11.85	0.47	0.72	0.97	0.00	0.97	0.00	0.17
12.56	0.51	0.81	0.94	0.00	0.94	0.00	0.18
13.65	0.62	0.96	0.96	0.00	0.96	0.00	0.09
14.61	0.71	1.10	0.96	0.00	0.96	0.00	0.09
15.70	0.87	1.27	1.03	0.00	1.03	0.00	0.05
16.98	1.05	1.49	1.06	0.00	1.06	0.00	0.03
17.95	1.31	1.66	1.18	0.00	1.18	0.00	0.05

LIST OF REFERENCES

1. Stokes, G. G., "On the Effect of the Internal Friction of Fluids on the Motion of Pendulums", Proceedings of the Cambridge Philosophical Society, v. 1, part 7, p. 104-106, 9 December 1850.

2. Morison, J. R., O'Brien, M. P., Johnson, J. W., and Schaaf, S. A., "The Force Exerted by Surface Waves on Piles". Journal of Petroleum Technology, American Institute of Mining and Metallurgical Engineers, v. 189, p. 149-154, May 1950.

3. Keulegan, G. H., and Carpenter, L. H., "Forces on Cylinders and Plates in an Oscillating Fluid", Journal of Research of the National Bureau of Standards, v. 60, no. 5, p. 423-440, May 1958.

4. Heinzer, A. J., "Experimental Investigation of the Wake of an Oscillating Cylinder", unpublished Master's Thesis, University of Houston, Houston, Texas, 1968.

5. Sarpkaya, T., and Garrison, C. J., "Vortex Formation and Resistance in Unsteady Flow", Journal of Applied Mechanics Transactions of the ASME, v. 30, series E, no. 1, p. 16-24, March 1963.

6. Ward, E. G., and Dalton, C., "Strictly Sinusoidal Flow Around a Stationary Cylinder", Journal of Basic Engineering, v. 91, no. 4, p. 707-713, December 1969.

7. Bryson, A. E., Jr., "Symmetric Vortex Separation on Circular Cylinders and Cones", Journal of Applied Mechanics Transactions of the ASME, v. 81, series E, no. 4, p. 643-648, December 1959.

8. Dalton, C., and Hamann, F., "The Forces on a Cylinder Oscillating Sinusoidally in Water", ASME Paper no. 71-PET-2.

9. Schiller, F. C., "Wave Forces on a submerged Horizontal Cylinder", unpublished Master's Thesis, Unites States Naval Postgraduate School, Monterey, California, 1971.

INITIAL DISTRIBUTION LIST

		No. Copies
1.	Defense Documentation Center Cameron Station Alexandria, Virginia 22314	2
2.	Library, Code 0212 Naval Postgraduate School Monterey, California 93940	2
3.	Assistant Professor C. J. Garrison, Code 59Gm Department of Mechanical Engineering Naval Postgraduate School Monterey, California 93940	2
4.	Assistant Professor E. B. Thornton, Code 58Tm Department of Oceanography Naval Postgraduate School Monterey, California 93940	1
5.	LT Richard L. Gosselin, USN NAVSHIPREPFAC, GUAM FPO San Francisco, California 96630	2
6.	Department of Mechanical Engineering, Code 59 Naval Postgraduate School Monterey, California 93940	1

Security Classification

DOCUMENT CONTROL DATA - R & D

(Security classification of title, body of abstract and indexing annotation must be entered when the overall report is classified)

ORIGINATING ACTIVITY (Corporate author)

Naval Postgraduate School
Monterey, California 93940

2a. REPORT SECURITY CLASSIFICATION: Unclassified

2b. GROUP:

REPORT TITLE

Added Mass of a Circular Cylinder Under a Free Surface

DESCRIPTIVE NOTES (Type of report and inclusive dates)

Master's Thesis, December 1971

AUTHOR(S) (First name, middle initial, last name)

Richard Leon Gosselin

REPORT DATE: December 1971

7a. TOTAL NO. OF PAGES: 76

7b. NO. OF REFS: 9

8a. CONTRACT OR GRANT NO.:

b. PROJECT NO.:

c.:

d.:

9a. ORIGINATOR'S REPORT NUMBER(S):

9b. OTHER REPORT NO(S) (Any other numbers that may be assigned this report):

10. DISTRIBUTION STATEMENT

Approved for public release; distribution unlimited.

11. SUPPLEMENTARY NOTES:

12. SPONSORING MILITARY ACTIVITY

Naval Postgraduate School
Monterey, California 93940

13. ABSTRACT

When a circular cylinder is immersed in a fluid of infinite extend and oscillated in such a manner that drag effects are negligible, it is well-known that the closed form solution gives an added mass coefficient of 1.0. However, when boundaries are placed in proximity to the cylinder, and the cylinder oscillated parallel to the boundary, the added mass varies from the classical result. The forces acting on the cylinder in the latter case are dependent upon the proximity of the boundaries as well as the frequency of oscillation.

It was the purpose of this study to experimentally determine the total force on such a cylinder in proximity to an impermeable bottom surface and under a free surface and to relate this force to the added mass coefficient. Experimental data was reduced using a computer program and the results presented graphically as a function of dimensionless parameters.

DD FORM 1 NOV 65 1473 (PAGE 1)

S/N 0101-807-6811

Security Classification

A-31408

KEY WORDS	LINK A		LINK B		LINK C	
	ROLE	WT	ROLE	WT	ROLE	WT
Added Mass						
Circular Cylinder						
Free Surface						

Thesis
G583
c.1

133839

Gosselin
Added mass of a
circular cylinder
under a free surface.